Table 1.1 Historic Landmarks in Organotransition Metal Chemistry

Year	Event	Reference
1827	Zeise's salt discovered, $K^+[(C_2H_4)PtCl_3]$.	[29]
1868	Schutzenberger prepared the first carbonyl complex, $[PtCl_2(CO)_2]$.	[30]
1890	Mond prepares $Ni(CO)_4$.	[31]
1891	Mond and Berthelot prepare $Fe(CO)_5$.	[32]
1919	Hein prepares ill characterized η^6-arene chromium compounds.	[33]
1925	The Fischer-Tropsch process is developed.	[36]
1930	Reihlen prepares 1,3-butadiene-iron tricarbonyl.	[37]
1938	Roelen discovers the cobalt-catalyzed oxo-process.	[38]
1938	Calvin discovers homogeneous catalytic hydrogenation of quinone by copper acetate.	[21]
1938	Lucas and Winstein study silver-olefin complexes.	[39]
1939	Iguchi describes a rhodium-based homogeneous hydrogenation catalyst.	[41]
1938–1945	Reppe's group develops many homogeneously catalyzed processes.	[42]
1948	Reppe describes the catalytic cyclotrimerization of acetylene to cyclooctatetraene.	[43]
1951	Orgel, Pauling, and Zeiss describe the backbonding in metal carbonyls.	[44]
1951	Ferrocene is discovered by Kealy and Pauson and by Miller.	[45]
1952	Wilkinson, Rosenblum, Whiting, and Woodward propose a sandwich structure for ferrocene.	[46]
1952	E.O. Fischer describes the cobalticenium cation.	[47]

from Collman, Hegedus, Norton & Finke p.13 f

1955	Cotton and Wilkinson discover fluxional behavior.	[49]
1955	Halpern begins to study the mechanism of homogeneous catalytic hydrogenation.	[50]
1955	Ziegler and Natta discover metal-catalyzed olefin polymerization.	[51]
1956	Longuet-Higgins and Orgel predict stable cyclobutadiene complexes.	[52]
1958	The structure of $[CpMo(CO)_3]_2$ reveals a covalent metal-metal bond without bridging ligands.	[54]
1958	Criegee and Hubel prepare stable cyclobutadiene complexes.	[53]
1959	Shaw and Chatt describe an oxidative-addition reaction.	[56]
1961	Crowfoot-Hodgkin elucidates the structure of the coenzyme vitamin B_{12}.	[58]
1962	Vaska discovers the "Vaska Complex."	[57]
1964	Fischer isolates the first carbene complex.	[59]
1964	Banks reports olefin metathesis.	[60]
1965	Allen and Senoff discover the first dinitrogen complex.	[61]
1965	Wilkinson and Coffey independently discover "the Wilkinson Hydrogenation Complex."	[62a,b]
1969	Whitesides develops a direct NMR method for discovering the stereochemistry at carbon of organometallic reactions.	
1971	Monsanto develops rhodium-catalyzed acetic acid process.	[63]
1973	E.O. Fischer prepares the first complex having a metal-carbon triple bond.	[65]
1974	Commercial synthesis of L-Dopa by asymmetric catalytic hydrogenation.	[1]
1975	DuPont's adiponitrile synthesis by catalytic addition of HCN to butadiene.	[70]
1978	Tebbe discovers "the Tebbe reagent."	[71]
1980	Brown [67] and Halpern [68] independently elucidate the mechanism of asymmetric catalytic olefin hydrogenation.	[67,68]
1981	Schrock discovers a homogeneous catalyst for acetylene metathesis.	[66]
1982	Bergman describes intermolecular oxidative-addition of saturated hydrocarbons.	[72a]
1983	Watson [73] and Graham [74] independently report the activation of methane by oxidative-addition.	[73,74]
1983	The concept of "agostic" structures is formulated by Brookhart and Green.	[74]
1983	Phosphines are reported to degrade during catalytic hydroformylation.	[76]

The 16 and 18 Electron Rule in Organometallic Chemistry and Homogeneous Catalysis

The 16 and 18 Electron Rule.-Two postulates or rules for organometallic complexes and their reactions are proposed.

1. Diamagnetic organometallic complexes of transition metals may exist in a significant concentration at moderate temperatures only if the metal's valence shell contains 16 or 18 electrons. A significant concentration is one that may be detected spectroscopically or kinetically and may be in the gaseous, liquid, or solid state.
2. Organometallic reactions, including catalytic ones, proceed by elementary steps involving only intermediates with 16 or 18 metal valence electrons.

from C. A. Tolman, *Chemical Society Reviews*, **1972**, *1*, 337.

In the following table, ligands commonly encountered in organotransition-metal chemistry are listed together with the respective numbers of electrons relevant to the application of the 18 VE rule:

Neutral	Positive	Negative	Ligand L
1	0	2	alkyl, aryl, hydride, halide (X)
2	–	–	ethylene, monoolefin, CO, phosphane etc.
3	2	4	π-allyl, enyl, cyclopropenyl, NO
4	–	–	diolefin
4	–	6	cyclobutadiene (C_4H_4 or $C_4H_4^{2-}$)
5	–	6	cyclopentadienyl, dienyl
6	–	–	arene, triolefin
7	6	–	tropylium ($C_7H_7^+$)
8	–	10	cyclooctatetraene (C_8H_8 or $C_8H_8^{2-}$)

. The following table lists the more important organic ligands containing at least two carbon atoms, which coordinate to the transition metal through σ bonds:

Carbon Hybridization	Ligand: terminal		Ligand: bridging	
sp^3	$M-CR_3$	Alkyl	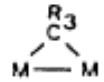	3-Center μ_2-alkyl
			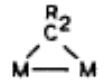	μ_2-Alkylidene
			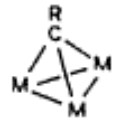	μ_3-Alkylidyne
sp^2	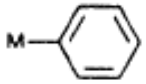	Aryl		3-Center μ_2-aryl
	$M=CR_2$	Carbene or alkylidene	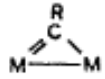	μ_2-Alkylidyne
	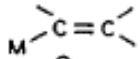	Vinyl	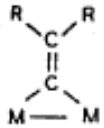	μ_2-Vinylidene
	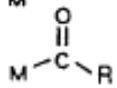	Acyl		
sp	$M\equiv CR$	Carbyne or alkylidyne	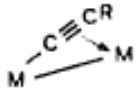	$\mu_2(\sigma,\pi)$-Alkynyl
	$M-C\equiv CR$	Alkynyl		
	$M=C=CR_2$	Vinylidene	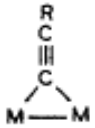	3-Center μ_2-alkynyl

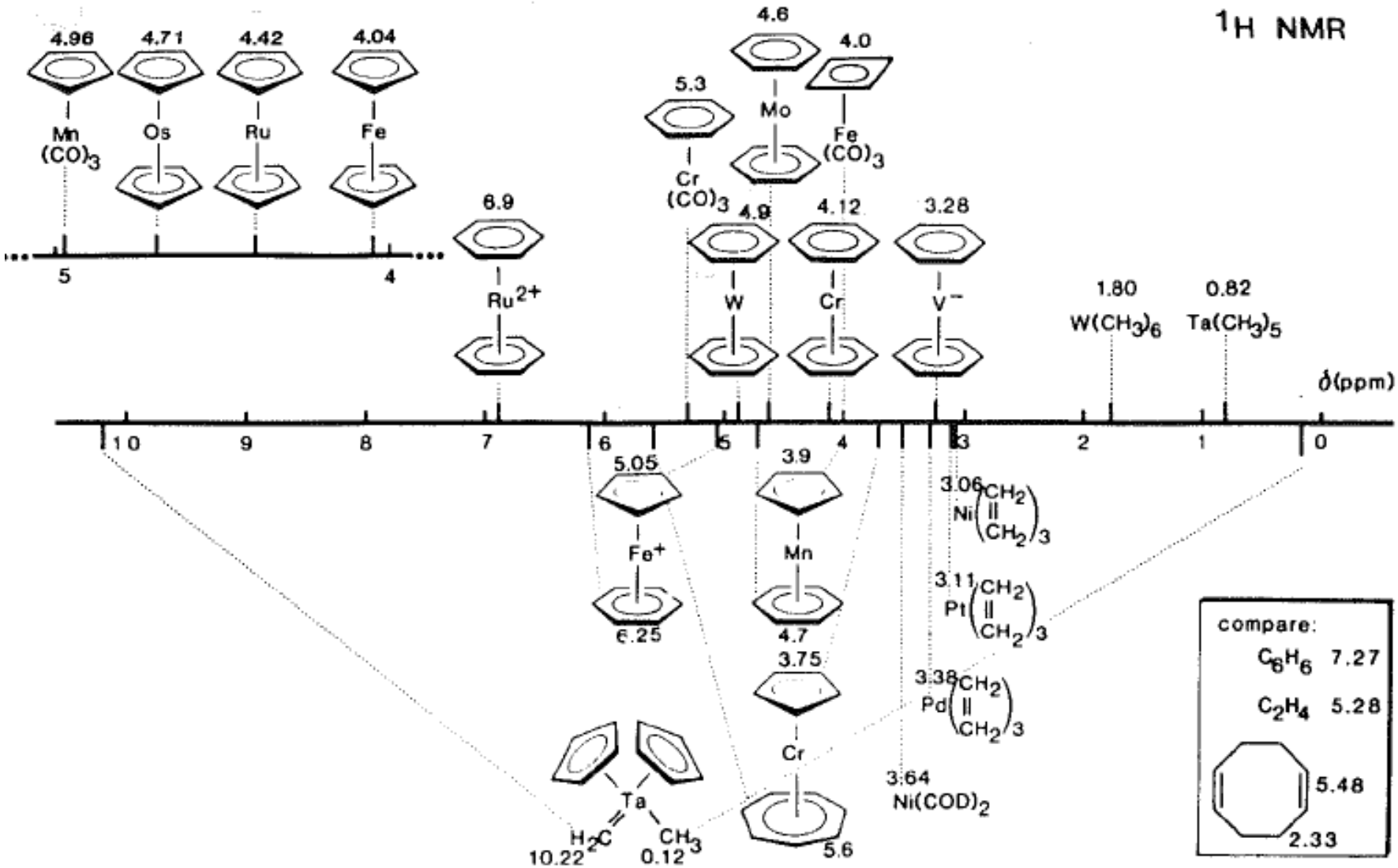

Figure 15-4: δ ^{1}H values for diamagnetic organotransition-metal compounds.

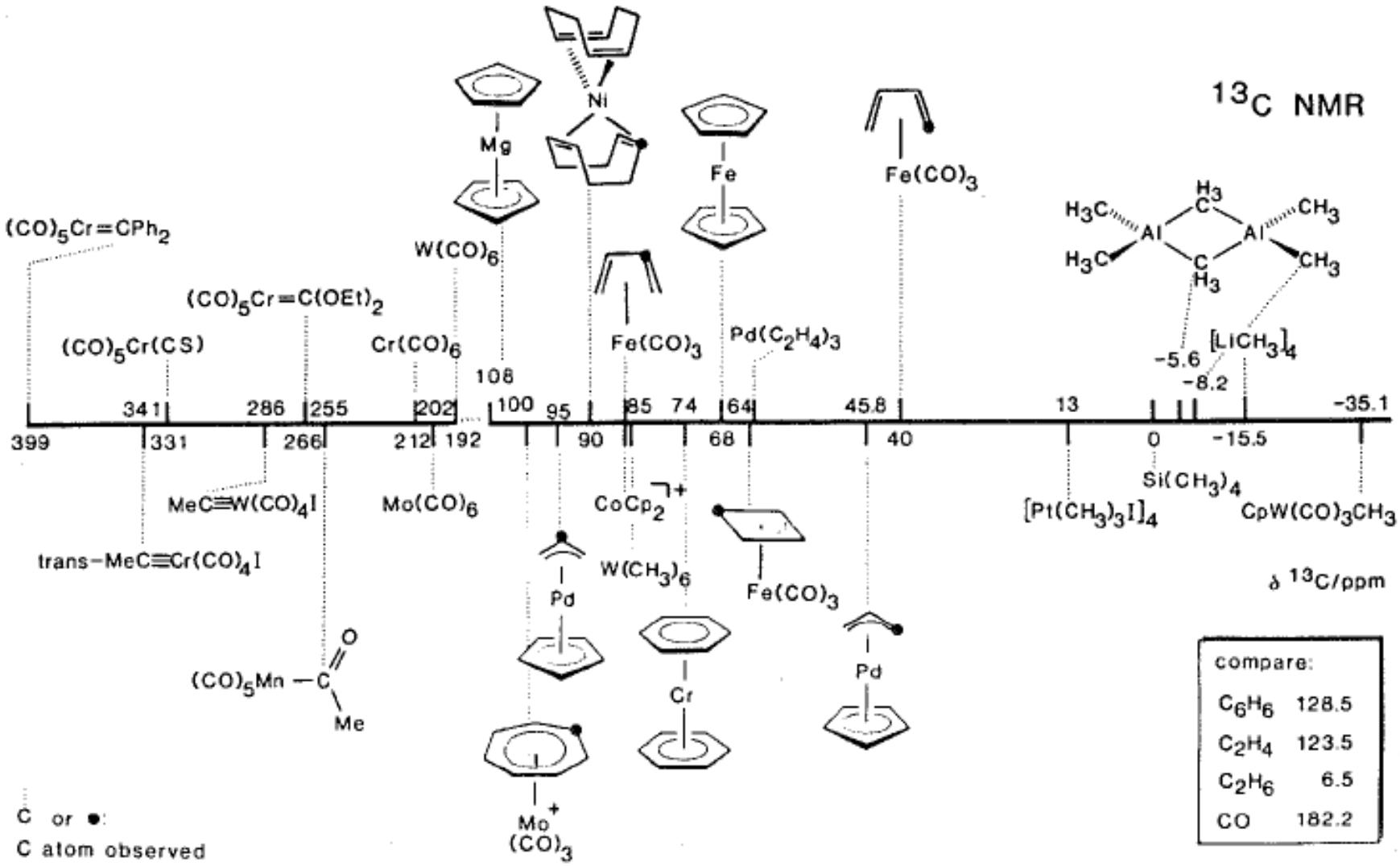

Figure 15-1: Survey of δ ^{13}C values for metal-coordinated carbon atoms of various classes of organometallic compounds.

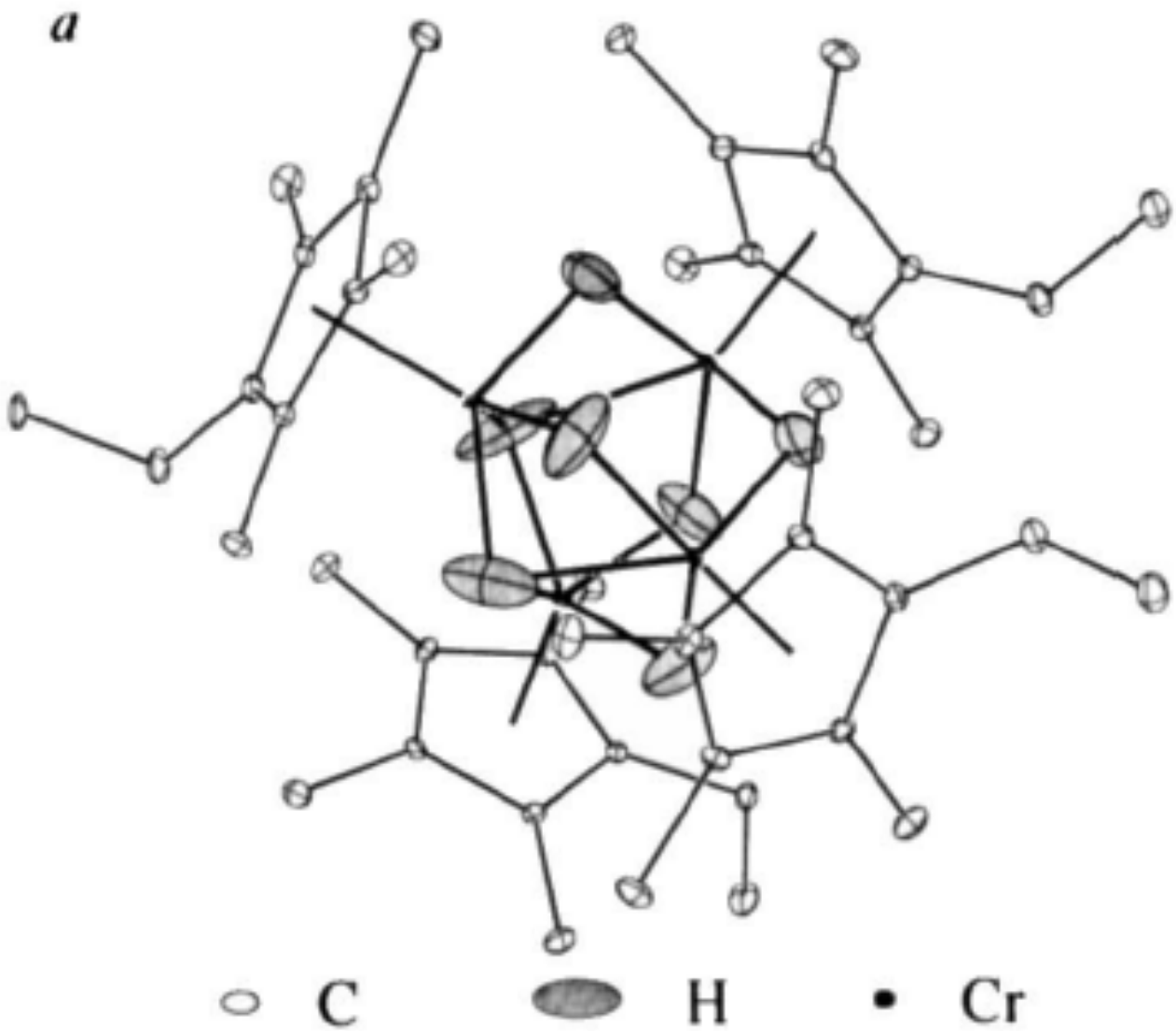

R. A. Heintz et al, *Nature* **1995**, *378*, 359

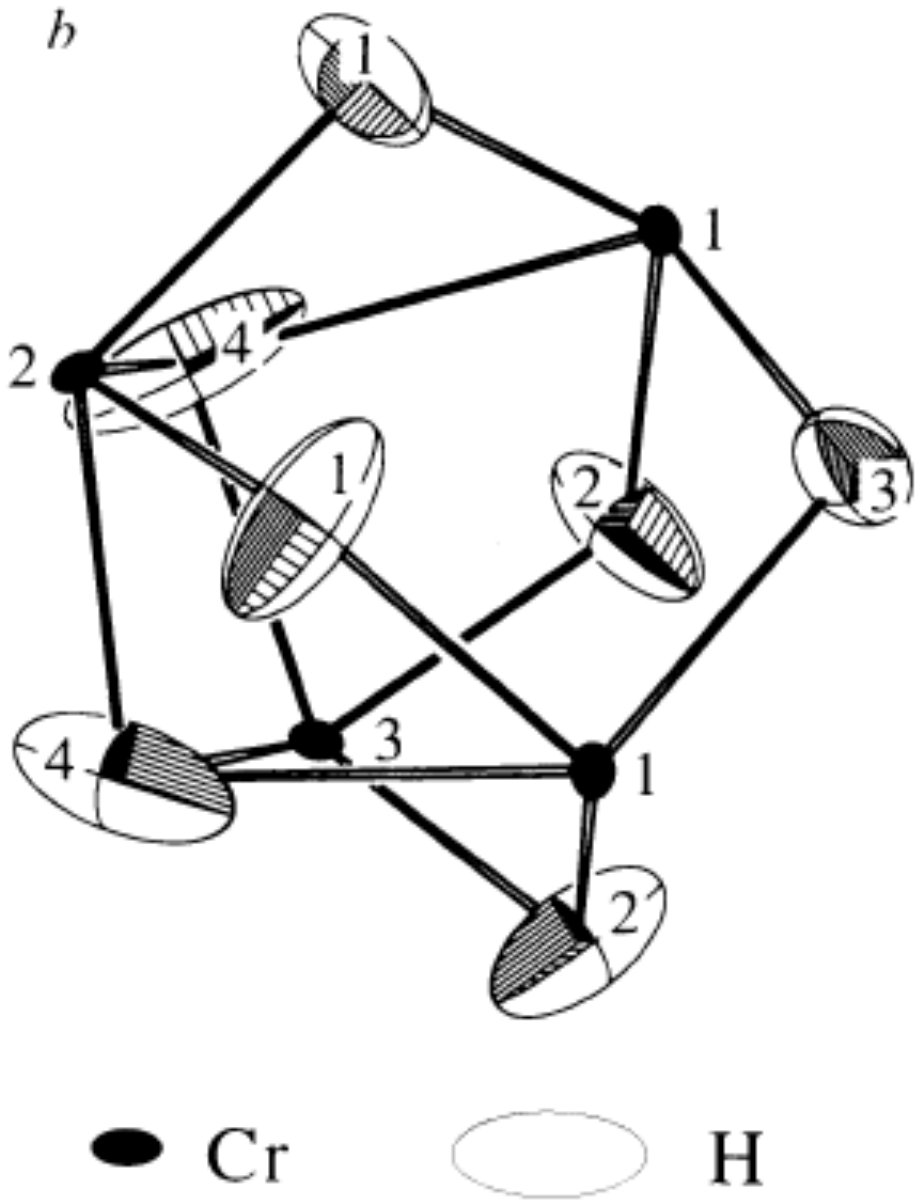
b
1
1
2
4
1
2
3
4
3
1
2
Cr
H

M-H distance by neutron diffraction

Table 17
Average M–H bond lengths in all compounds [a]

	V	Cr	Mn	Fe	Co	Ni	Cu
Terminal			1.606(16)	**1.575(17)**			
Bridging (μ_2)		**1.728(5)**	1.719(5)	**1.664(11)**	1.641(6)		
Face-bridging (μ_3)		1.753(7)			**1.734(3)**	**1.691(7)**	1.77(3)
Ternary			1.756(2)	**1.580(5)**	**1.568(9)**	**1.590(10)**	
	Nb	**Mo**	**Tc**	**Ru**	**Rh**	**Pd**	**Ag**
Terminal		1.737(5)		**1.611(7)**	**1.566(3)**		
Bridging (μ_2)		**1.841(12)**		**1.782(4)**	**1.774(3)**		1.831(5)
Face-bridging (μ_3)					1.859(6)		
Ternary				**1.706(5)**	**1.690(14)**	**1.656(17)**	
	Ta	**W**	**Re**	**Os**	**Ir**	**Pt**	**Au**
Terminal	**1.783(6)**	**1.743(6)**	**1.679(4)**	**1.649(4)**	**1.590(6)**	1.610(2)	
Bridging (μ_2)		**1.891(30)**	**1.837(8)**	**1.814(4)**	**1.809(15)**	1.697(15)	
Face-bridging (μ_3)				**1.889(16)**			
Ternary			1.724(4)	**1.723(18)**	**1.688(9)**	**1.628(5)**	

R. Bau, *Inorg. Chim. Acta*, **1997**, *259*, 27

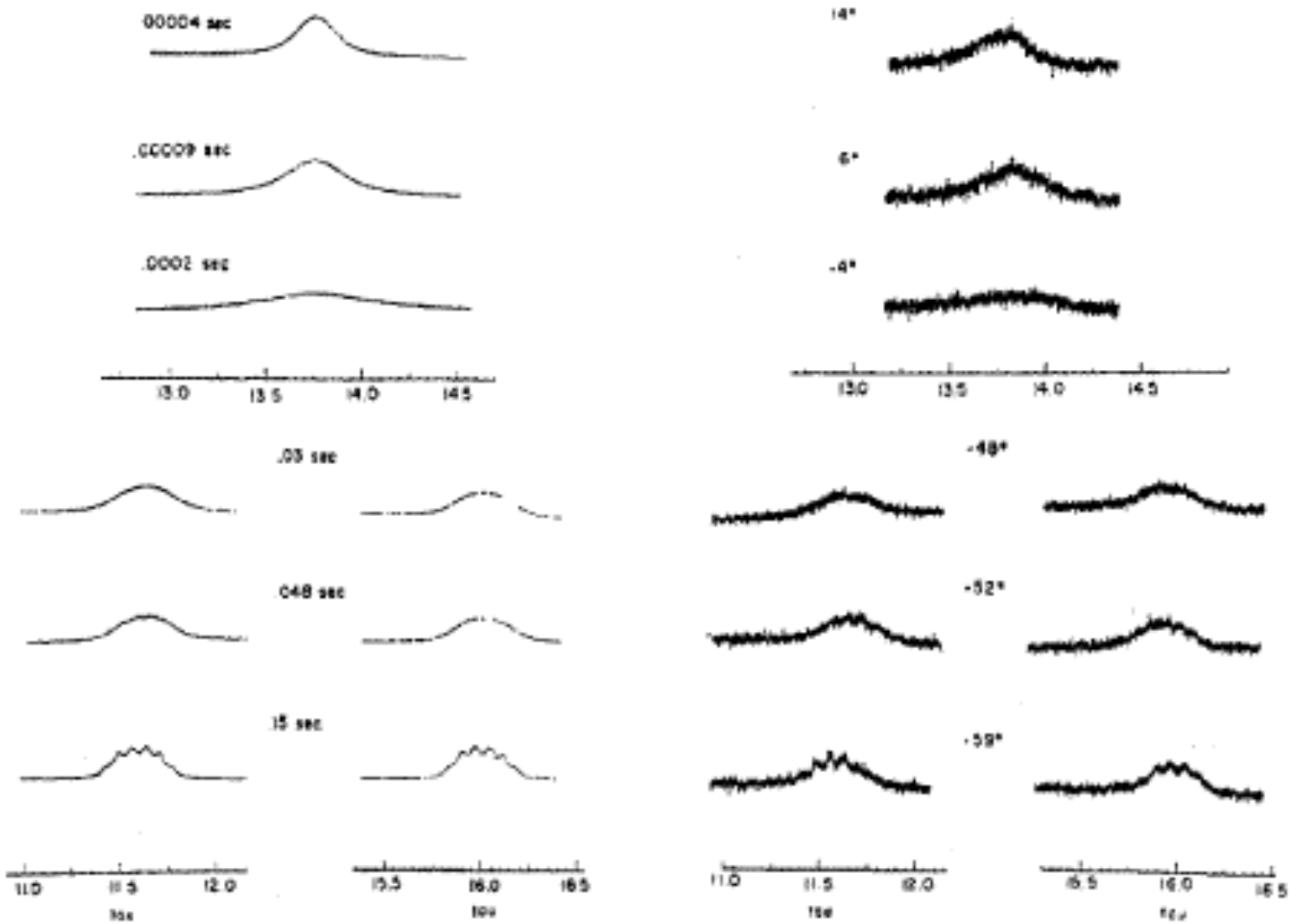

Figure 1. The 100-MHz pmr spectra at several temperatures of the upfield methylene region of $[Et_2B(pz)_2][\eta^3\text{-}CH_2C(Ph)CH_2](CO)_2Mo$ dissolved in $CF_2Cl_2 + CDCl_3 + CH_2Cl_2$ (5:5:2).

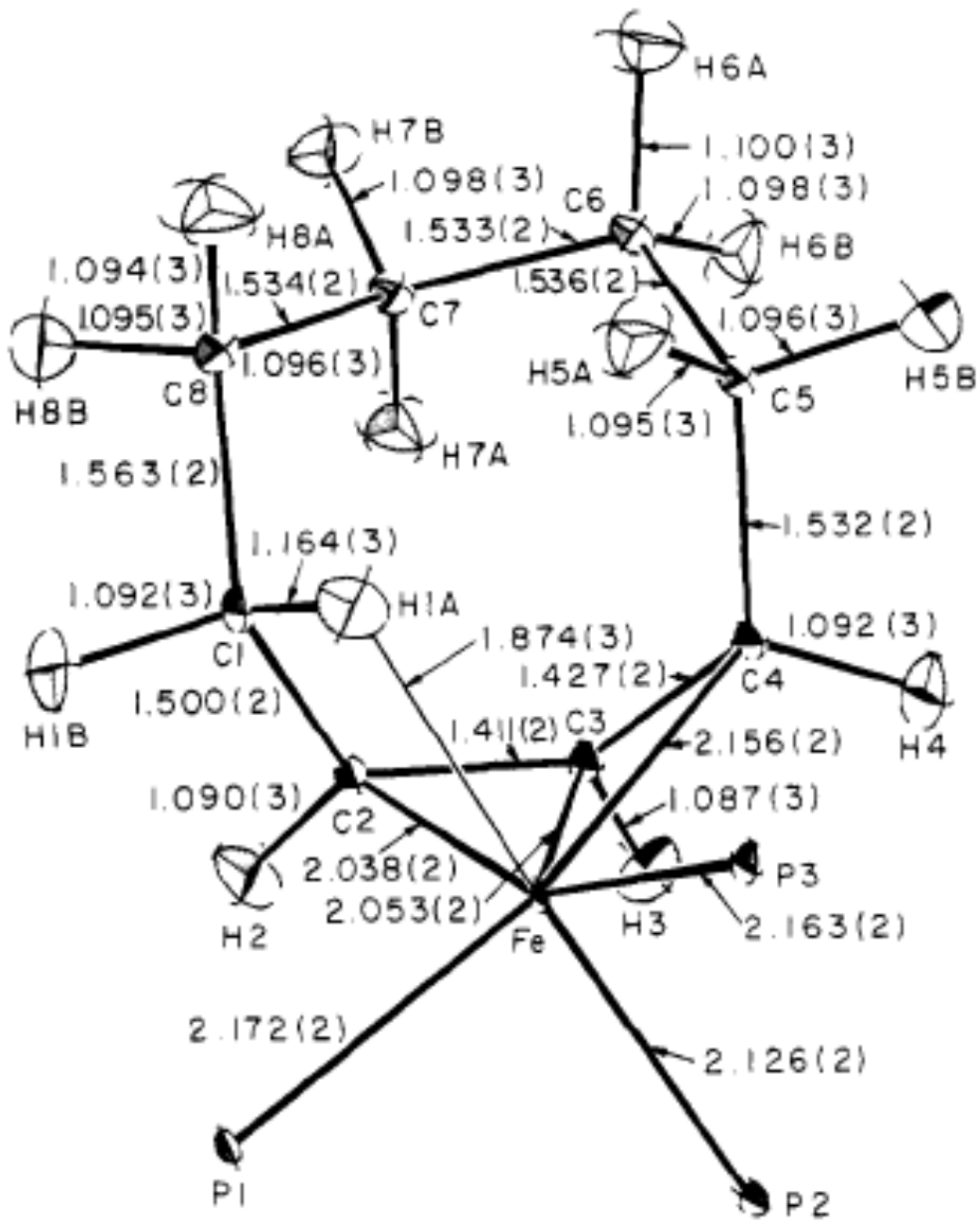
H6A
1.100(3)
H7B
1.098(3)
C6
1.098(3)
1.533(2)
H8A
H6B
1.094(3)
1.534(2)
1.536(2)
C7
1.095(3)
1.096(3)
H5A
H5B
H8B
C8
1.096(3)
C5
1.095(3)
H7A
1.563(2)
1.532(2)
1.164(3)
1.092(3)
H1A
1.092(3)
1.874(3)
C1
1.427(2)
C4
1.500(2)
H1B
1.411(2)
C3
2.156(2)
H4
1.090(3)
C2
1.087(3)
2.038(2)
P3
2.053(2)
H2
H3
2.163(2)
Fe
2.172(2)
2.126(2)
P1
P2

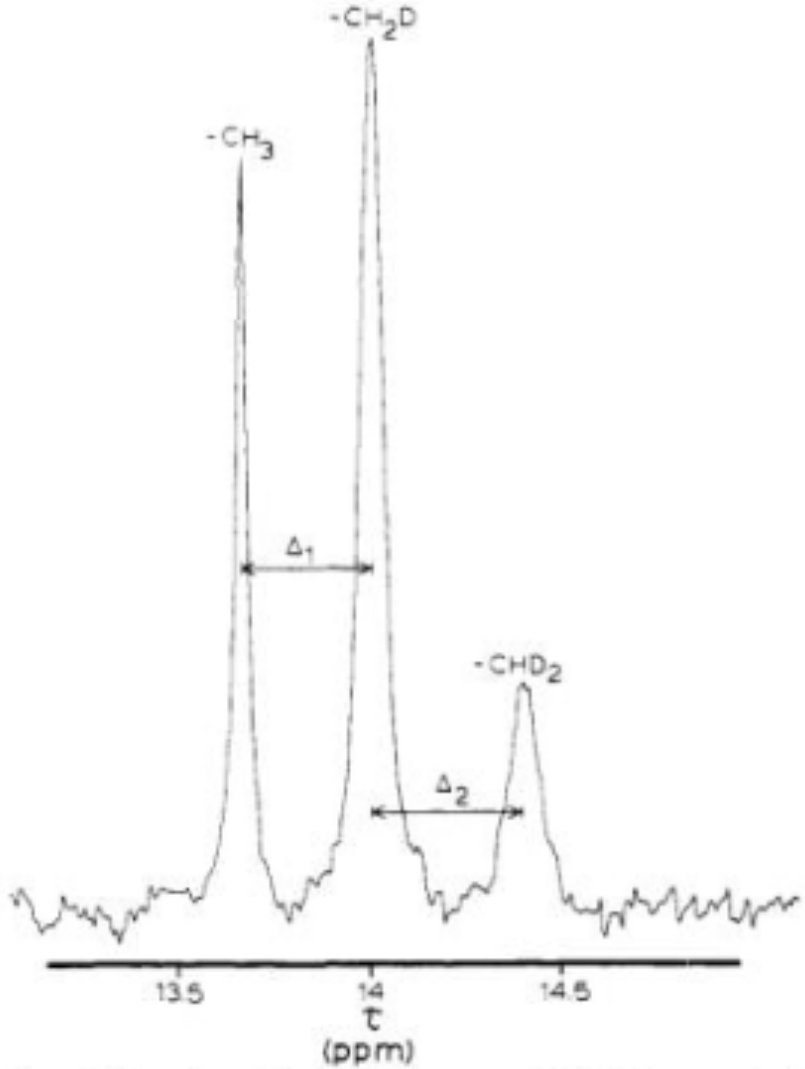

Figure 1. A portion of the ^{1}H NMR spectrum (35 °C) for a sample of "$Os_3(CO)_{10}CH_2D_2$", with some "$Os_3(CO)_{10}CH_4$" added as a reference.

Physical Properties of Selected Metal Carbonyls

Compound	Color	mp. in °C	Symmetry	IR ν_{CO} in cm^{-1}	Miscellaneous
$V(CO)_6$	green-black	70(*d*)	O_h	1976	paramagnetic, $S = 1/2$
$Cr(CO)_6$	white	130(*d*)	O_h	2000	$d(Cr-C) = 192$ pm $\Delta_o = 32'200\ cm^{-1}$
$Mo(CO)_6$	white	– (subl)	O_h	2004	$d(Mo-C) = 206$ pm $\Delta_o = 32'150\ cm^{-1}$
$W(CO)_6$	white	– (subl)	O_h	1998	$d(W-C) = 207$ pm $\Delta_o = 32'200\ cm^{-1}$
$Mn_2(CO)_{10}$	yellow	154	D_{4d}	2044(m) 2013(s) 1983(m)	$d(Mn-Mn) = 293$ pm
$Tc_2(CO)_{10}$	white	177	D_{4d}	2065(m) 2017(s) 1984(m)	
$Re_2(CO)_{10}$	white	177	D_{4d}	2070(m) 2014(s) 1976(m)	
$Fe(CO)_5$	yellow	–20	D_{3h}	2034(s) 2013(vs)	bp 103 °C, highly toxic $d(Fe-C_{ax}) = 181$ pm $d(Fe-C_{eq}) = 183$ pm
$Ru(CO)_5$	colorless	–22	D_{3h}	2035(s) 1999(vs)	unstable; forms $Ru_3(CO)_{12}$
$Os(CO)_5$	colorless	–15	D_{3h}	2034(s) 1991(vs)	very unstable; forms $Os_3(CO)_{12}$
$Fe_2(CO)_9$	gold-yellow	*d*	D_{3h}	2082(m) 2019(2) 1829(s)	$d(Fe-Fe) = 246$ pm
$Co_2(CO)_8$	orange red	51(*d*)	C_{2v} (solid) D_{3d} (solution)	 2112 2107 2071 2069 2059 2042 2044 2031 2031 2023 2001 1991 1886 1857	$d(Co-Co) = 254$ pm
$Ni(CO)_4$	colorless	–25	T_d	2057	bp 34 °C, highly toxic $d(Ni-C) = 184$ pm easily decomposes to Ni and 4 CO

15. Carbon Monoxide

Symmetry: $C_{\infty v}$

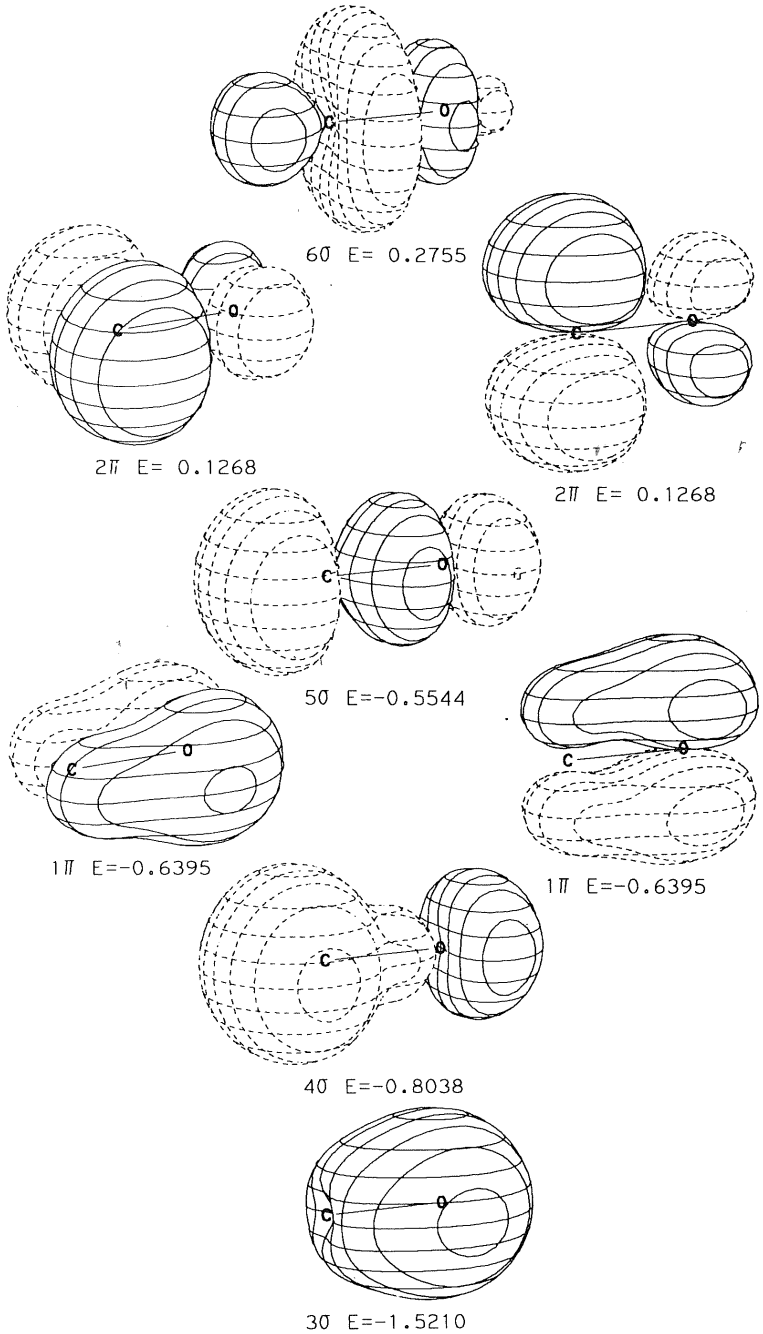

Number and Modes of IR-active bands (ν_{CO}) in carbonyl complexes, depending on the local symmetry of $M(CO)_n$

Complex	Number and Modes of IR-active Bands ν_{CO}	Point Group
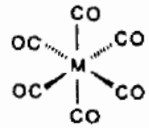 $M(CO)_6$	1 T_{1u}	O_h
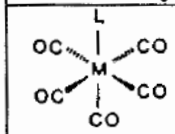 $LM(CO)_5$	3 $2A_1 + E$	C_{4v}
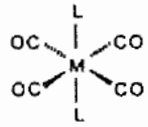 trans-$L_2M(CO)_4$	1 E_u	D_{4h}
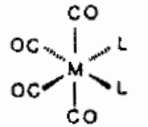 cis-$L_2M(CO)_4$	4 $2A_1 + B_1 + B_2$	C_{2v}
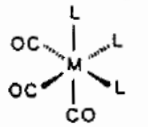 fac-$L_3M(CO)_3$	2 $A_1 + E$	C_{3v}
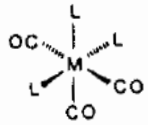 mer-$L_3M(CO)_3$	3 $2A_1 + B_2$	C_{2v}
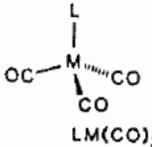 $LM(CO)_3$	2 $A_1 + E$	C_{3v}

Complex	Number and Modes of IR-active Bands ν_{CO}	Point Group
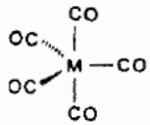 $M(CO)_5$	2 $A_2'' + E'$	D_{3h}
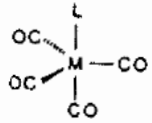 $LM(CO)_4$	3 $2A_1 + E$	C_{3v}
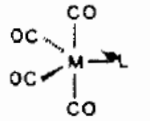 $LM(CO)_4$	4 $2A_1 + B_1 + B_2$	C_{2v}
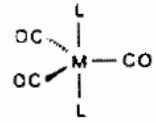 trans-$L_2M(CO)_3$	1 E'	D_{3h}
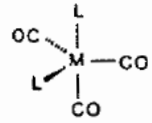 cis-$L_2M(CO)_3$	3 $2A' + A''$	C_s
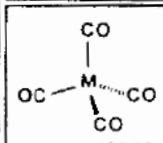 $M(CO)_4$	1 T_2	T_d
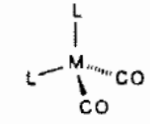 $L_2M(CO)_2$	2 $A_1 + B_1$	C_{2v}

18. Ethylene

Symmetry: D_{2h}

HOMO

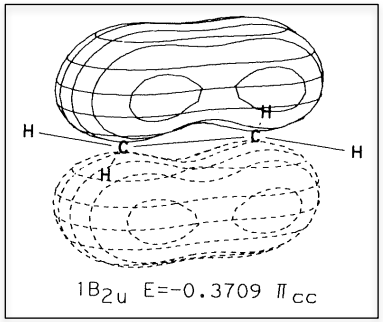

$1B_{2u}$ E=-0.3709 π_{CC}

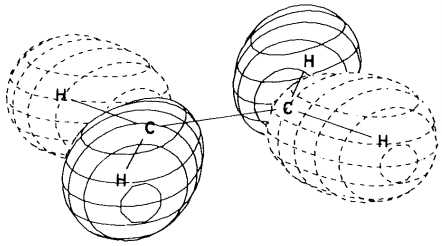

$1B_{2g}$ E=-0.5061 π'_{CH_2}

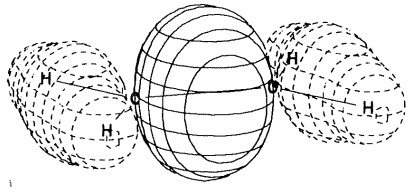

$3A_g$ E=-0.5616 σ_{CH_2}, σ_{CC}

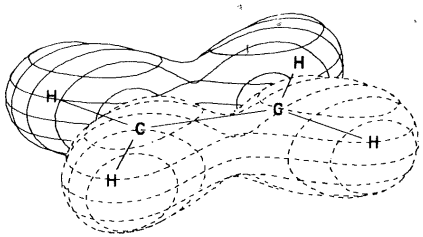

$1B_{3u}$ E=-0.6438 π'_{CH_2}

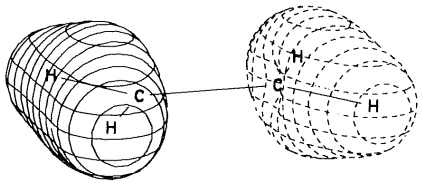

$2A_u$ E=-0.7823 σ_{CH_2}

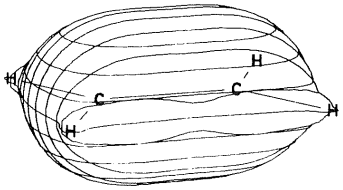

$2A_g$ E=-1.0144 σ_{CC}, σ_{CH_2}

Ethylene (Continued)

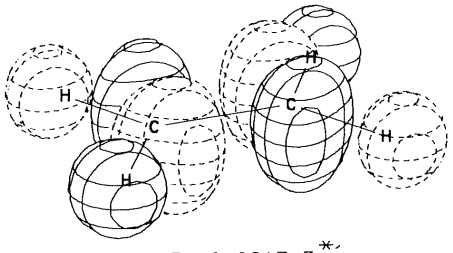

$2B_{2g}$ E= 0.8917 $\pi^{*}_{CH_2}$

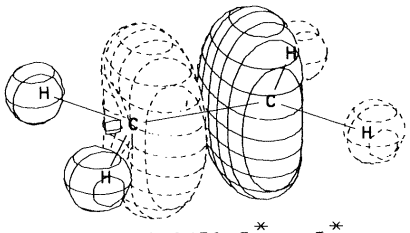

$4A_u$ E= 0.8453 σ^{*}_{CC}, $\sigma^{*}_{CH_2}$

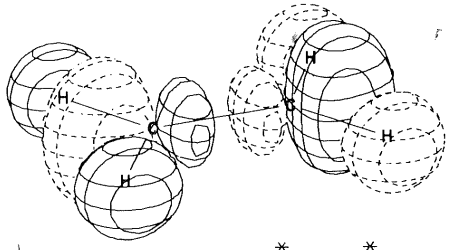

$3A_u$ E= 0.6395 $\sigma^{*}_{CH_2}$, σ^{*}_{CC}

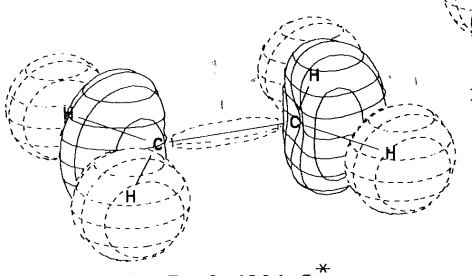

$4A_g$ E= 0.6206 $\sigma^{*}_{CH_2}$

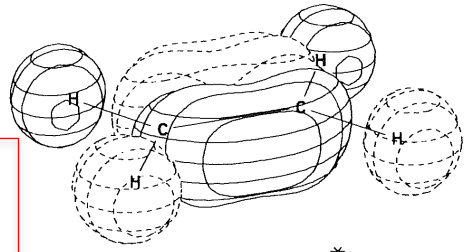

$2B_{3u}$ E= 0.5868 $\pi^{*}_{CH_2}$

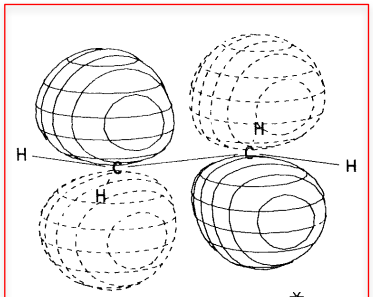

$1B_{3g}$ E= 0.2426 π^{*}_{CC}

LUMO

An unusual coordination mode for ethylene - μ-η^2:η^2-C_2H_4 !

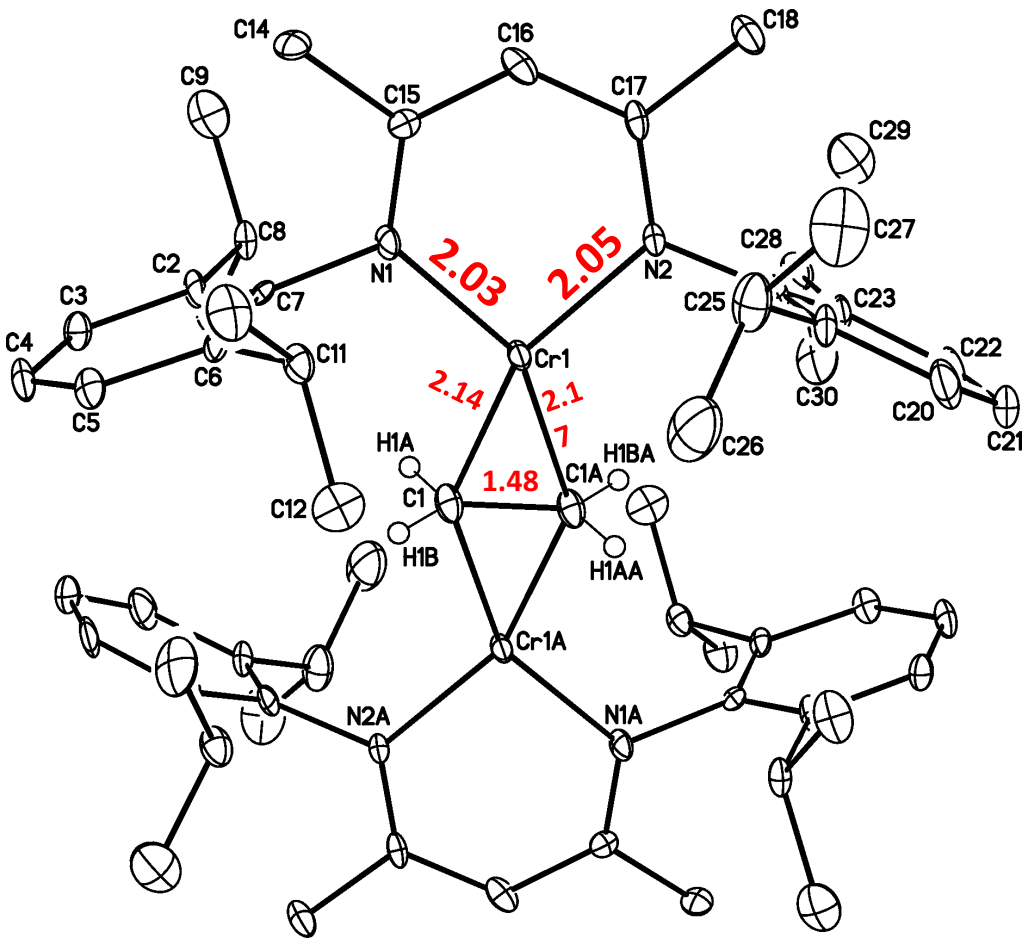

Related Compounds:

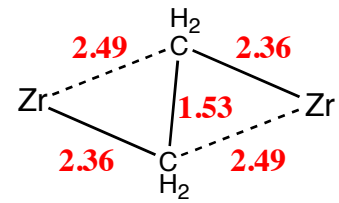

Kaminsky et al. *Angew. Chem. IEE* **1976**, *15*, 629

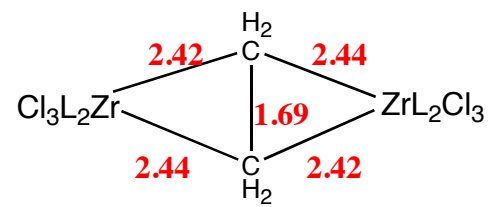

Cotton et al. *Polyhedron,* **1987**, *6*, 645

see F. A. Cotton *Inorg. Chem.* **2002**, *41*, 643
for a summary.

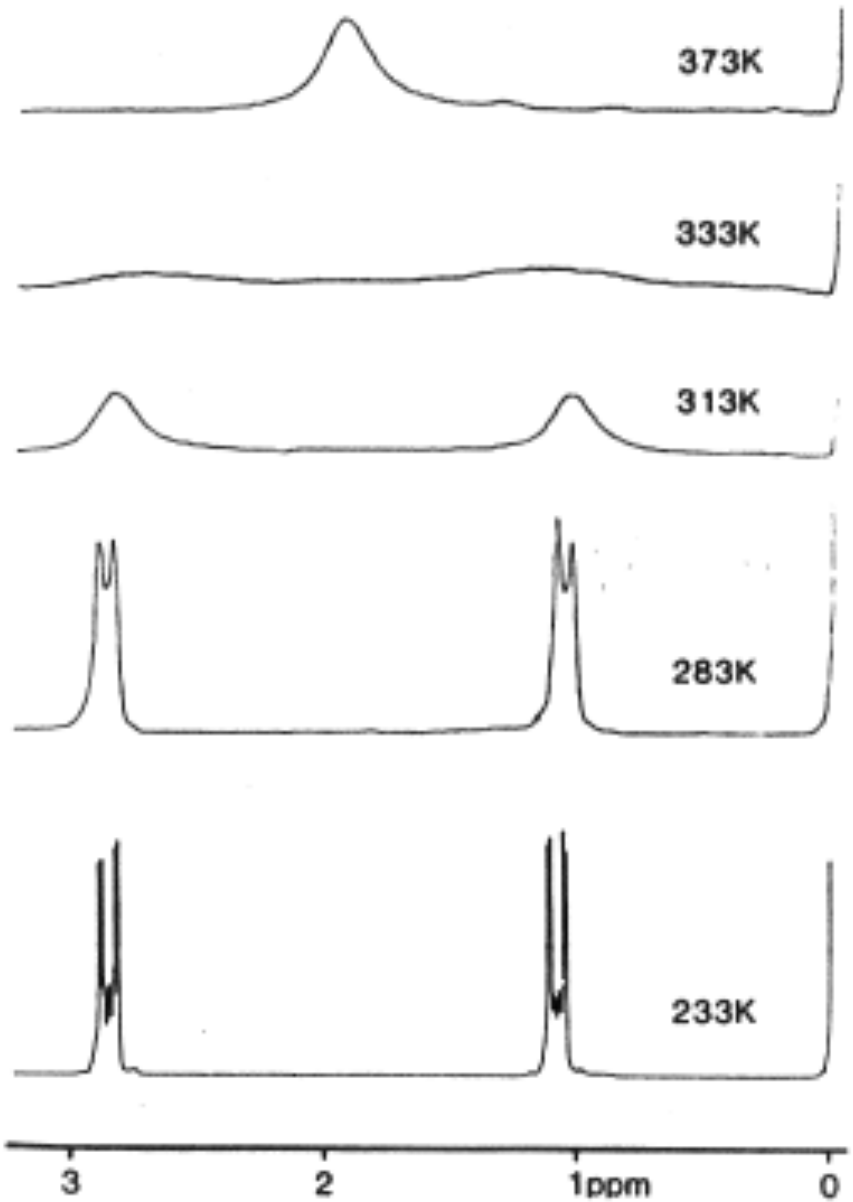

^{1}H-*NMR spectrum of* $C_5H_5Rh(C_2H_4)_2$ (200 MHz).

Intermediates on Ethylene Insertion Pathway into $[Cp(THF)Cr(n\text{-}Pr)]^+$

(DFT calculations - C. W. Hoganson et al., *Macromolecules* **2004**, *37*, 566**)**

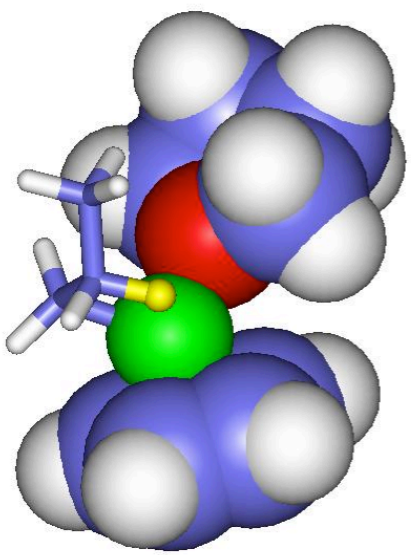

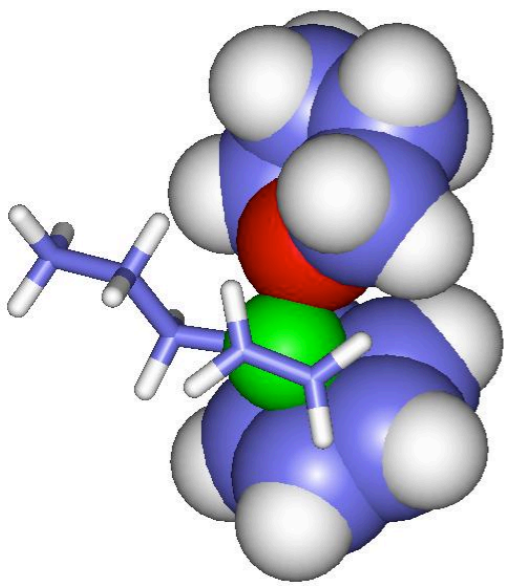

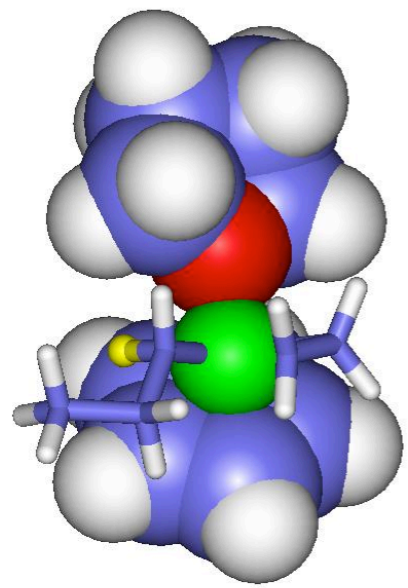

Reactant:

$Cr\text{-}C_\alpha$	2.03 Å
$Cr\text{-}H_\beta$	1.95 Å
$C_\beta\text{-}H_\beta$	1.165 Å

C_2H_4-complex:

$Cr\text{-}C_\alpha$	2.09 Å
$Cr\text{-}C_1$	2.66 Å
$Cr\text{-}C_2$	2.53 Å
$C_1\text{-}C_2$	1.37 Å
$C_\alpha\text{-}H$	1.11 Å

Transition State:

$Cr\text{-}C_\alpha$	2.23 Å
$Cr\text{-}C_1$	2.13 Å
$Cr\text{-}C_2$	2.38 Å
$C_1\text{-}C_2$	1.44 Å
$C_2\text{-}C_\alpha$	2.22 Å
$Cr\text{-}H_\alpha$	2.19 Å
$C_\alpha\text{-}H_\alpha$	1.12 Å

Gas phase free energy surface for ethylene/propene selectivity

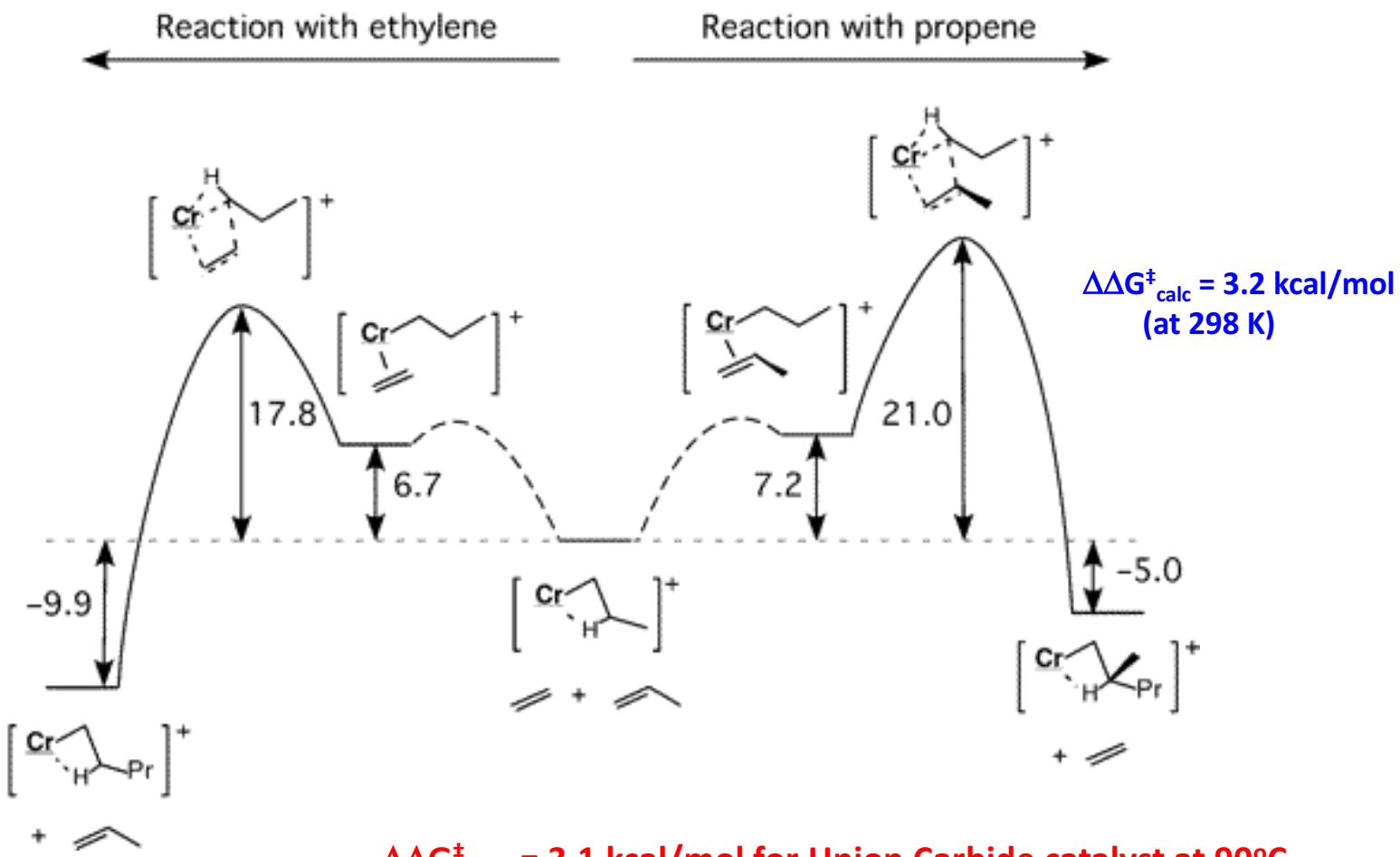

$\Delta\Delta G^{\ddagger}_{calc}$ = 3.2 kcal/mol (at 298 K)

$\Delta\Delta G^{\ddagger}_{expt}$ = 3.1 kcal/mol for Union Carbide catalyst at 90°C

H. Hoganson et al., *Macromolecules*, **2004**, *37*, 566.

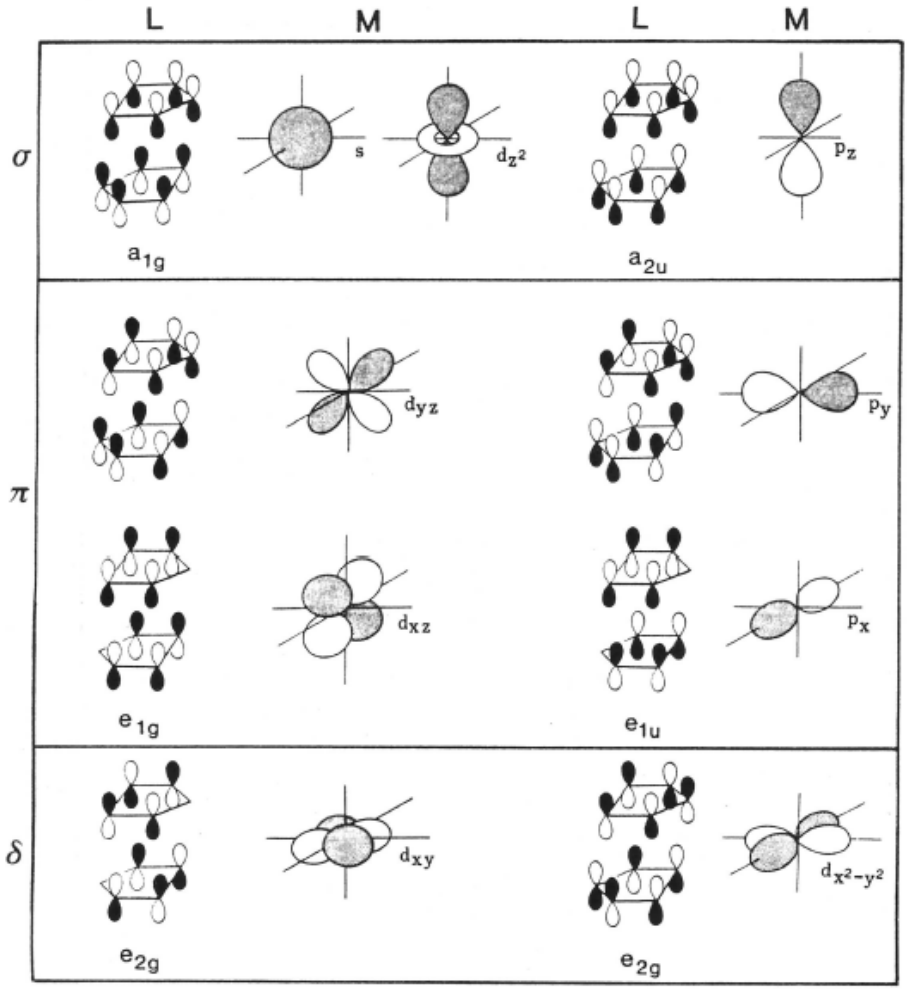
L
M
L
M
σ
π
δ
s
d_{z^2}
p_z
a_{1g}
a_{2u}
d_{yz}
p_y
d_{xz}
p_x
e_{1g}
e_{1u}
d_{xy}
$d_{x^2-y^2}$
e_{2g}
e_{2g}

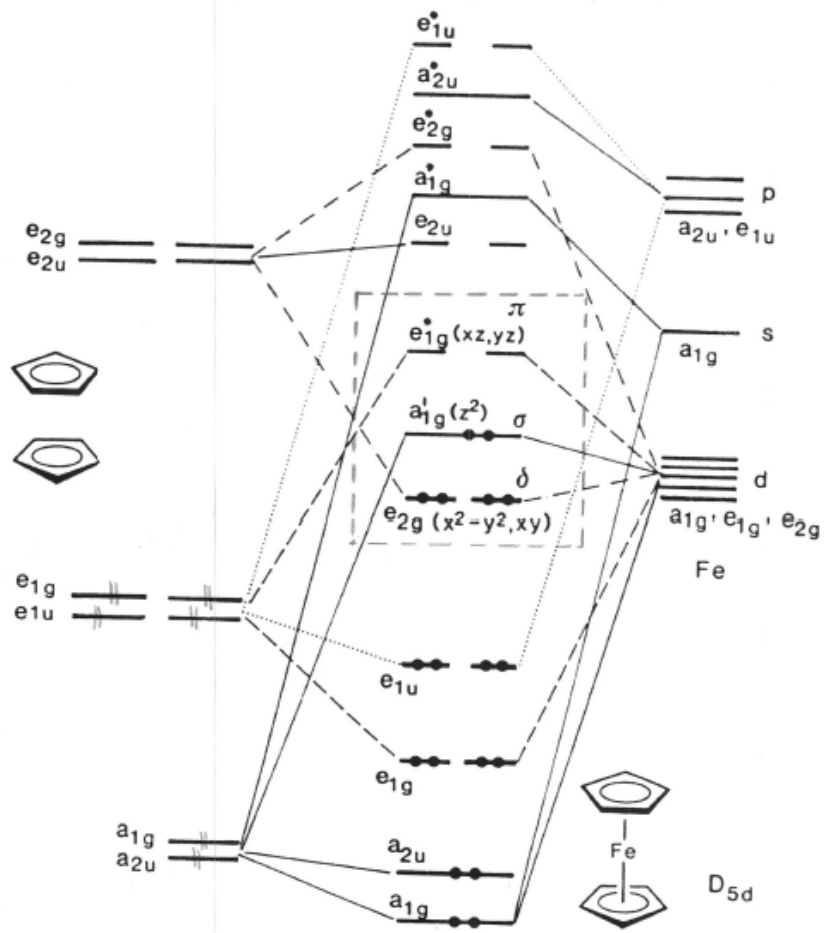
e^*_{1u}
a^*_{2u}
e^*_{2g}
a^*_{1g}
e_{2u}
e^*_{1g} (xz,yz)
π
a'_{1g} (z^2)
σ
δ
e_{2g} (x^2-y^2,xy)
e_{1u}
e_{1g}
a_{2u}
a_{1g}
e_{2g}
e_{2u}
e_{1g}
e_{1u}
a_{1g}
a_{2u}
p
a_{2u}, e_{1u}
s
a_{1g}
d
a_{1g}, e_{1g}, e_{2g}
Fe
Fe
D_{5d}

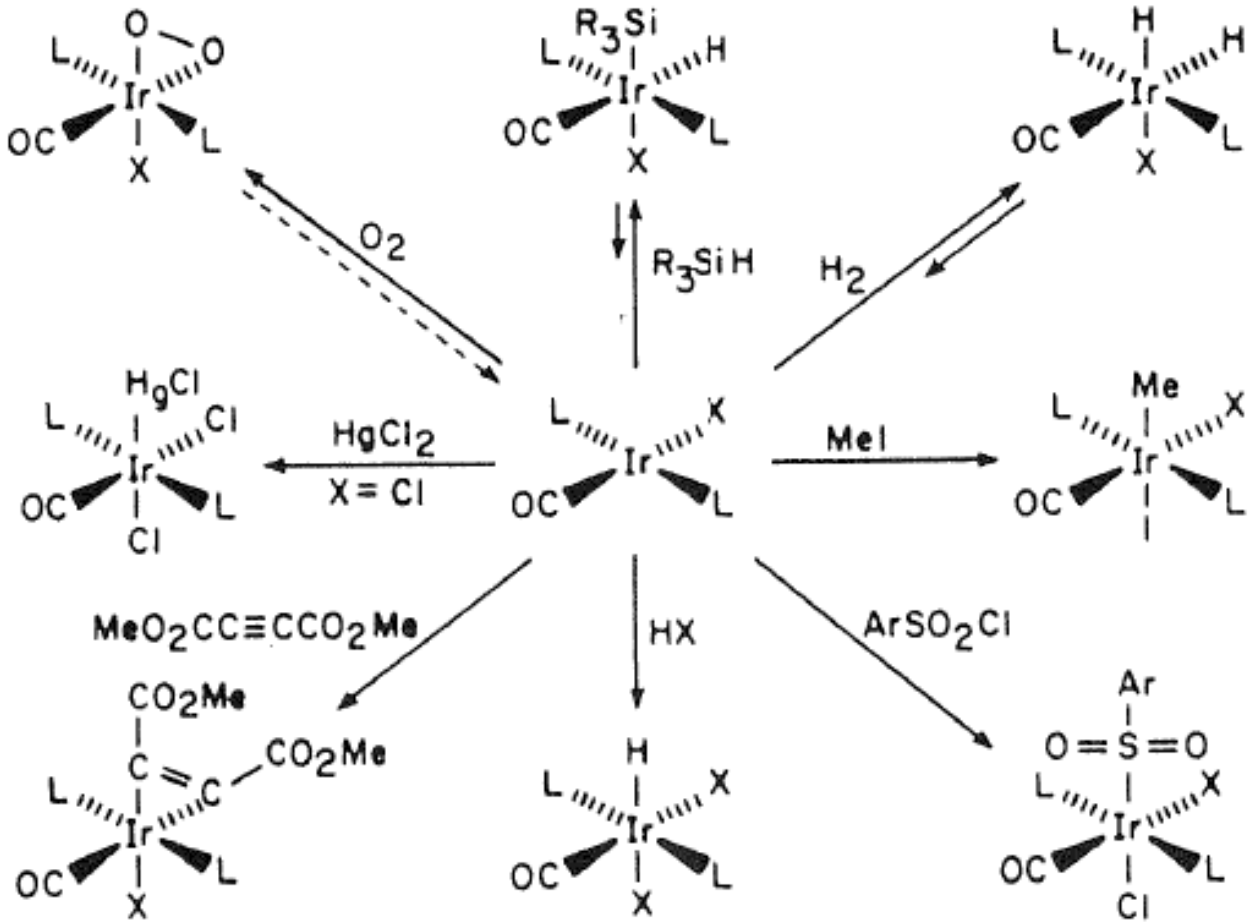

L. Vaska, *Acc. Chem. Res.* **1968**, *1*, 335

However, consider the oxidative addition of O_2 to Cr^I

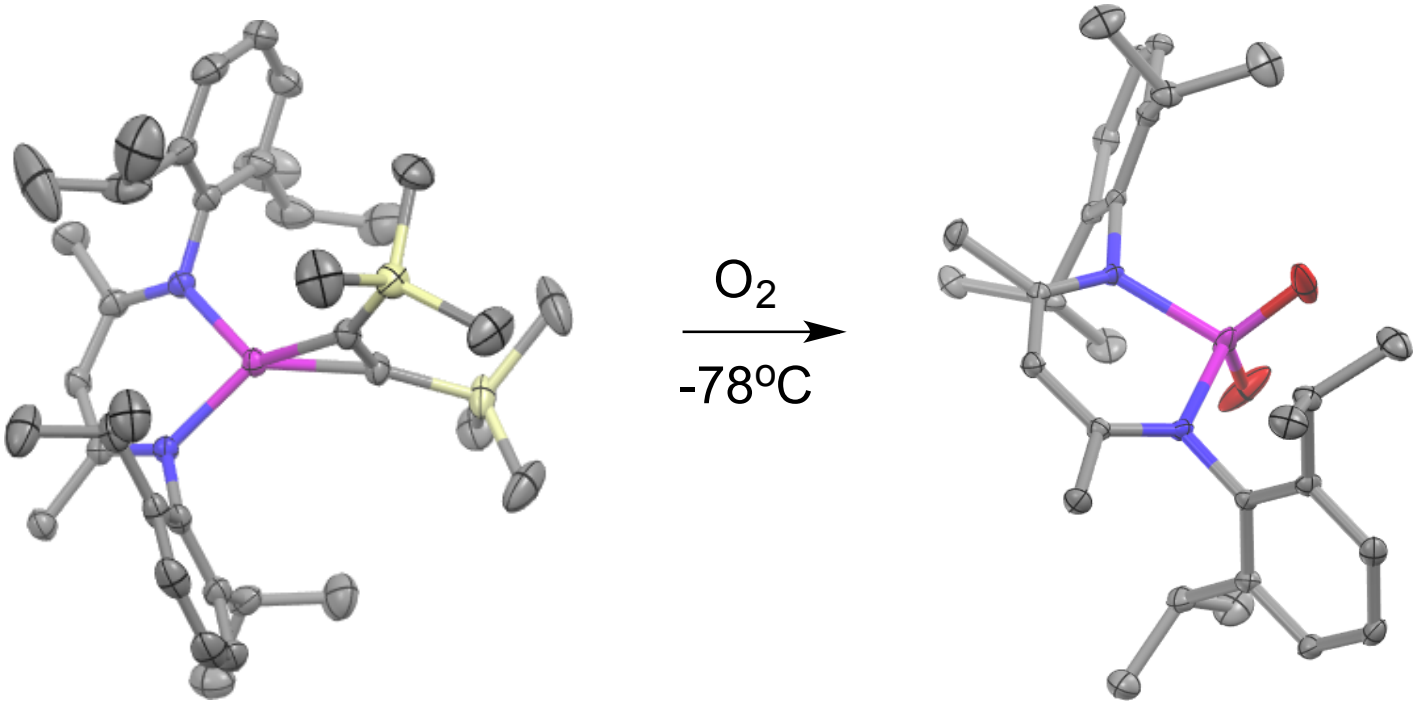

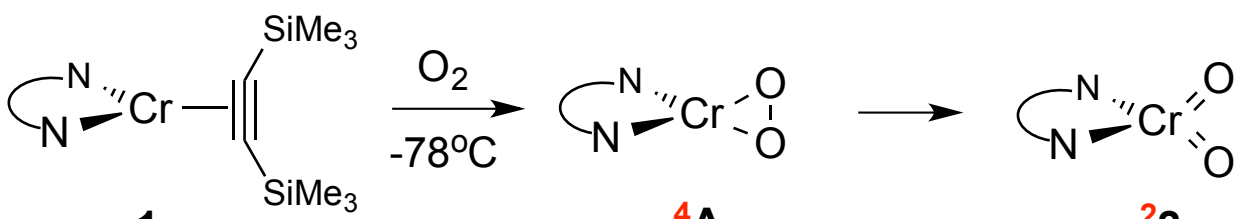

1 ^{4}**A** ^{2}**2**

F. Dai et al., *J. Am. Chem. Soc.* **2013**, *135*, 16774

A stable alkyl hydride of a first row transition metal!?

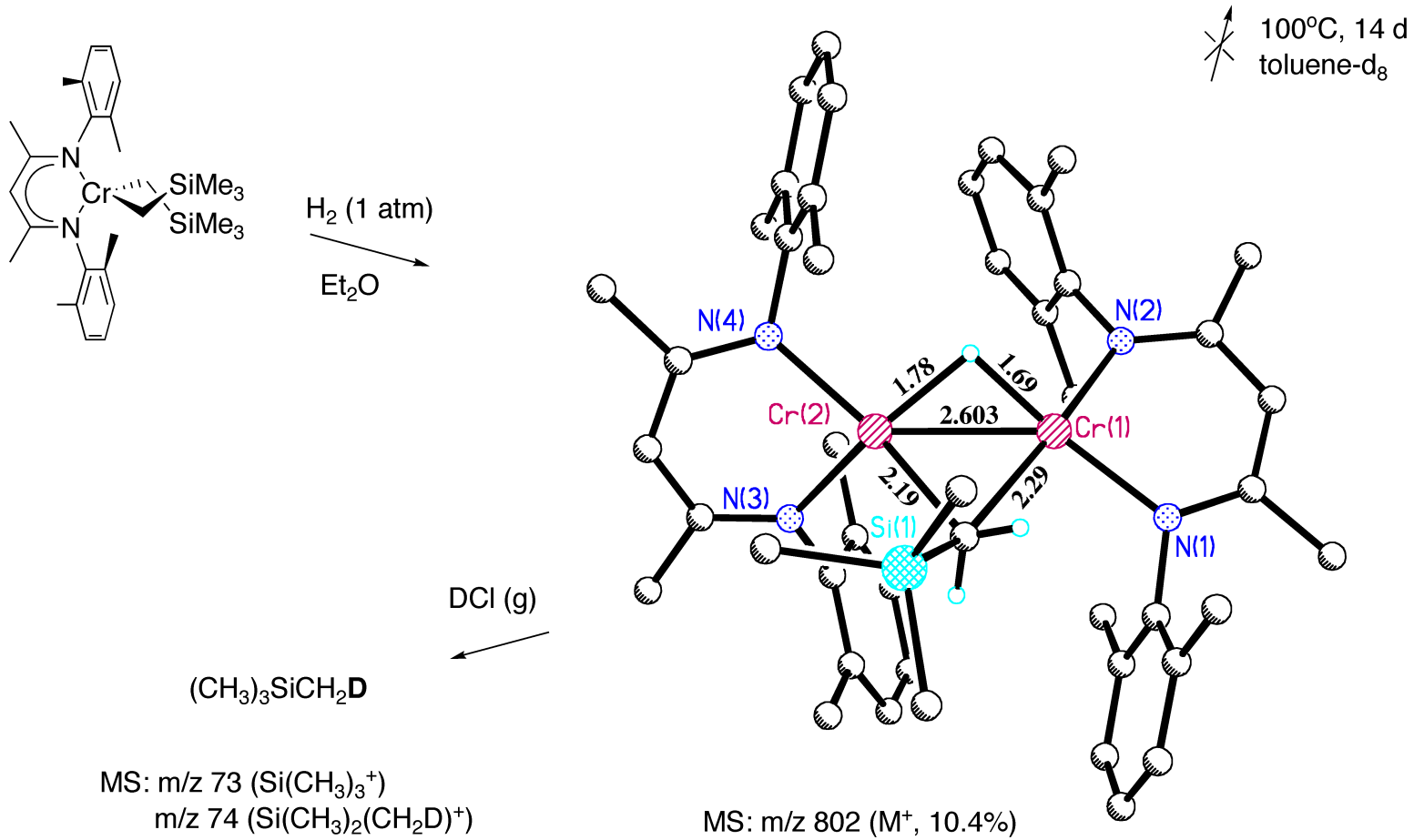

MS: m/z 73 ($Si(CH_3)_3^+$)
m/z 74 ($Si(CH_3)_2(CH_2D)^+$)

MS: m/z 802 (M^+, 10.4%)
μ_{eff} = 2.5 μ_B (1.8 μ_B/Cr)

L. A. MacAdams et al. *Chem. Commun.* **2003**, 1164

<u>Selective</u> oligomerization of ethylene via metallacycle intermediates

Scheme 1

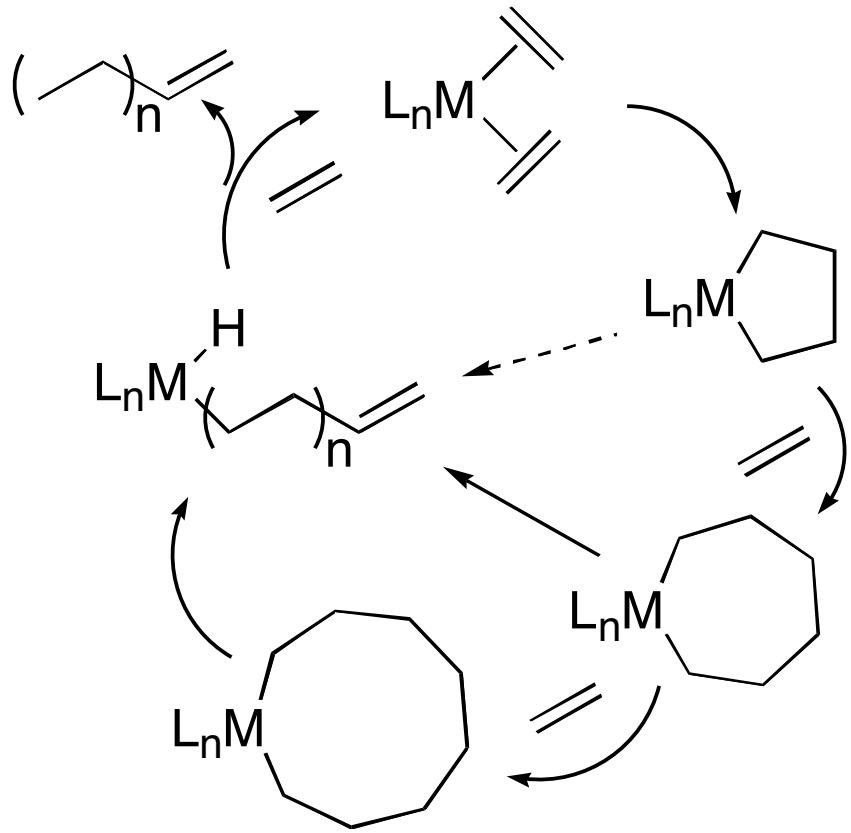

Recent review: J. T. Dixon, M. J. Green, F. M. Hess, D. H. Morgan, *JOMC* **2004**, *689*, 3641

Evidence for a Direct Bonding Interaction between Titanium and a β-C–H Moiety in a Titanium–Ethyl Compound; *X*-Ray Crystal Structure of $[Ti(Me_2PCH_2CH_2PMe_2)EtCl_3]$

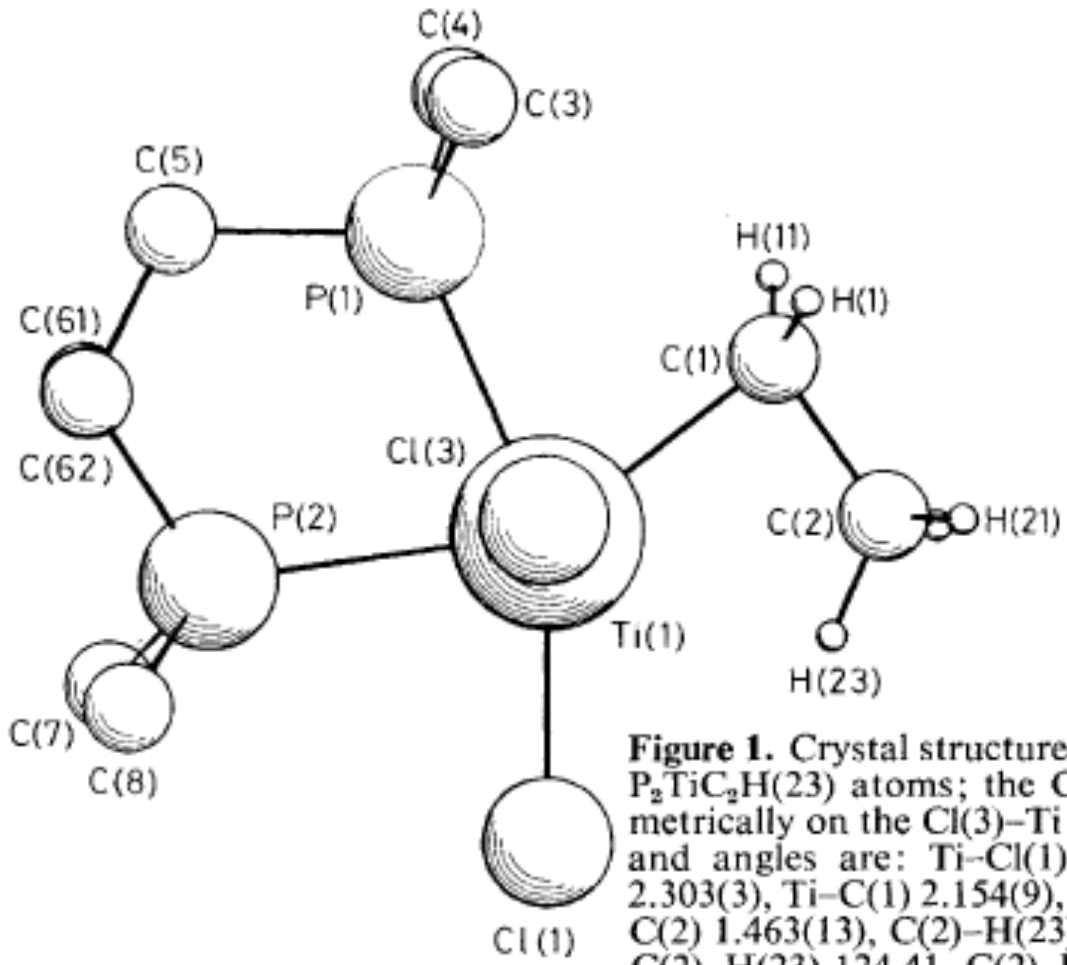

Figure 1. Crystal structure of (**1**) showing the plane containing the $P_2TiC_2H(23)$ atoms; the Cl(2) atom (not shown) is located symmetrically on the Cl(3)–Ti axis below the plane. Selected distances and angles are: Ti–Cl(1) 2.408(3), Ti–Cl(2) 2.313(3), Ti–Cl(3) 2.303(3), Ti–C(1) 2.154(9), Ti–C(2) 2.516(10), Ti–H(23) 2.29, C(1)–C(2) 1.463(13), C(2)–H(23) 1.02 Å; Ti–C(1)–C(2) 85.89(58), C(1)–C(2)–H(23) 124.41, C(2)–H(23)–Ti 90.4°.

The Synthesis and Structure of $[Co(\eta\text{-}C_5Me_5)Et\{P(p\text{-tolyl})_3\}]$ Cation: a Model for the β-Elimination Transition State

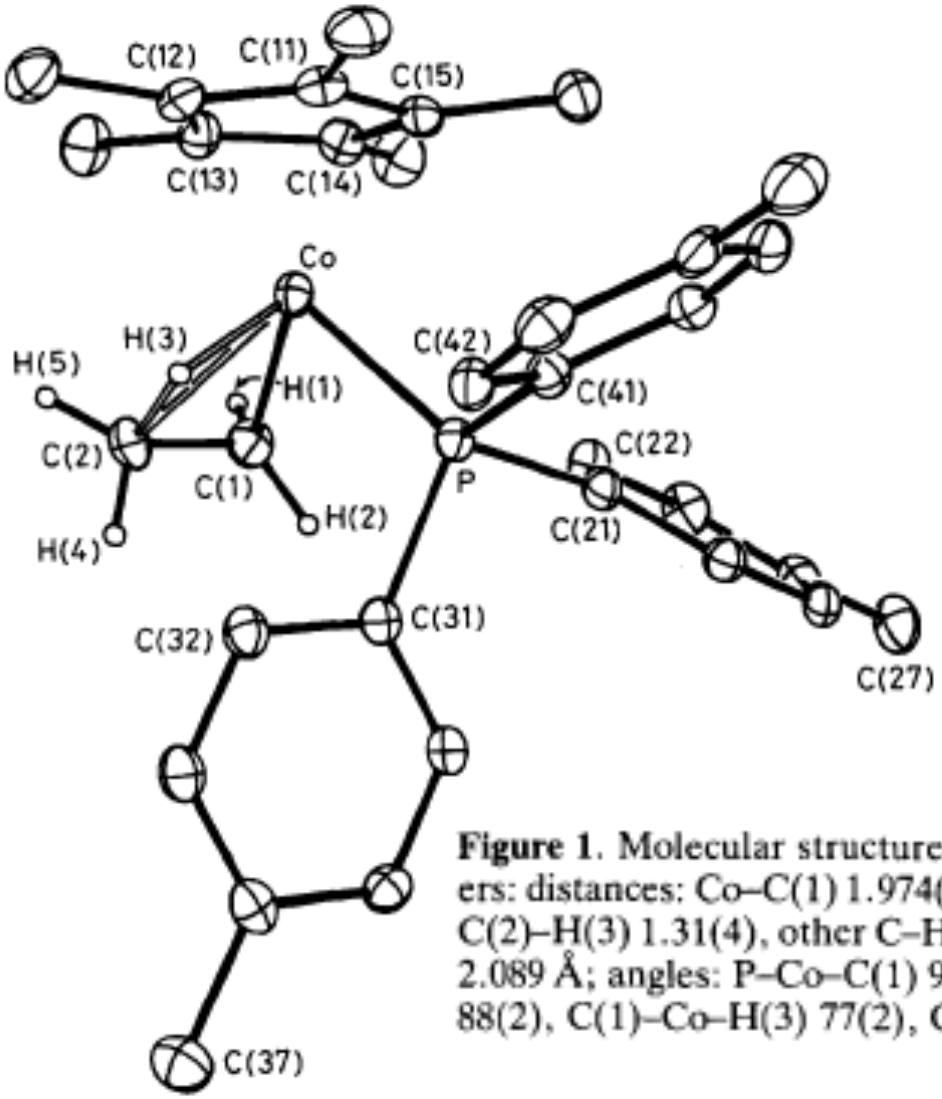

Figure 1. Molecular structure of (**2a**). Important molecular parameters: distances: Co–C(1) 1.974(4), Co–C(2) 2.128(4), Co–H(3) 1.46(4), C(2)–H(3) 1.31(4), other C–H 0.92(4)—0.98(4) Å, Co–C (C_5Me_5) av. 2.089 Å; angles: P–Co–C(1) 90.6(1), P–Co–C(2) 99.4(1), P–Co–H(3) 88(2), C(1)–Co–H(3) 77(2), Co–C(2)–C(1) 63.4(2)°.

$(2,6\text{-}^{i}Pr_2Ph)_2$nacnacCr catalyst produces branched homopolymer

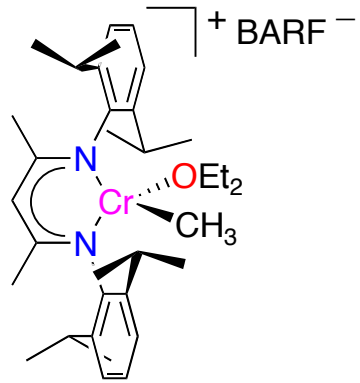

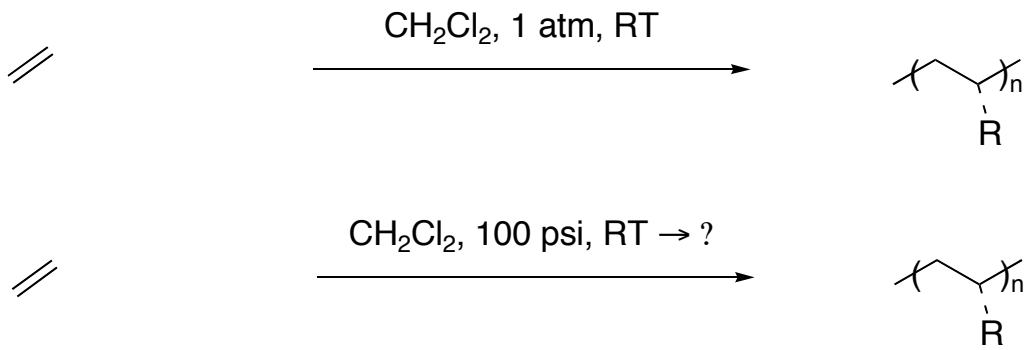

M_w = 6,500
M_n = 5,800
M_w/M_n = 1.12
8.9 Me/1000 C

M_w = 57,000
M_n =34,100
M_w/M_n = 1.67
25.8 Me/1000 C
2.1 Et/1000 C
1.2 Pr/1000 C
1.1 Bu/1000 C
0.3 Pe/1000 C

R = **H**, Me, Et, Pr, Bu,....

“Chain walk” depends on relative rate of insertion and isomerization

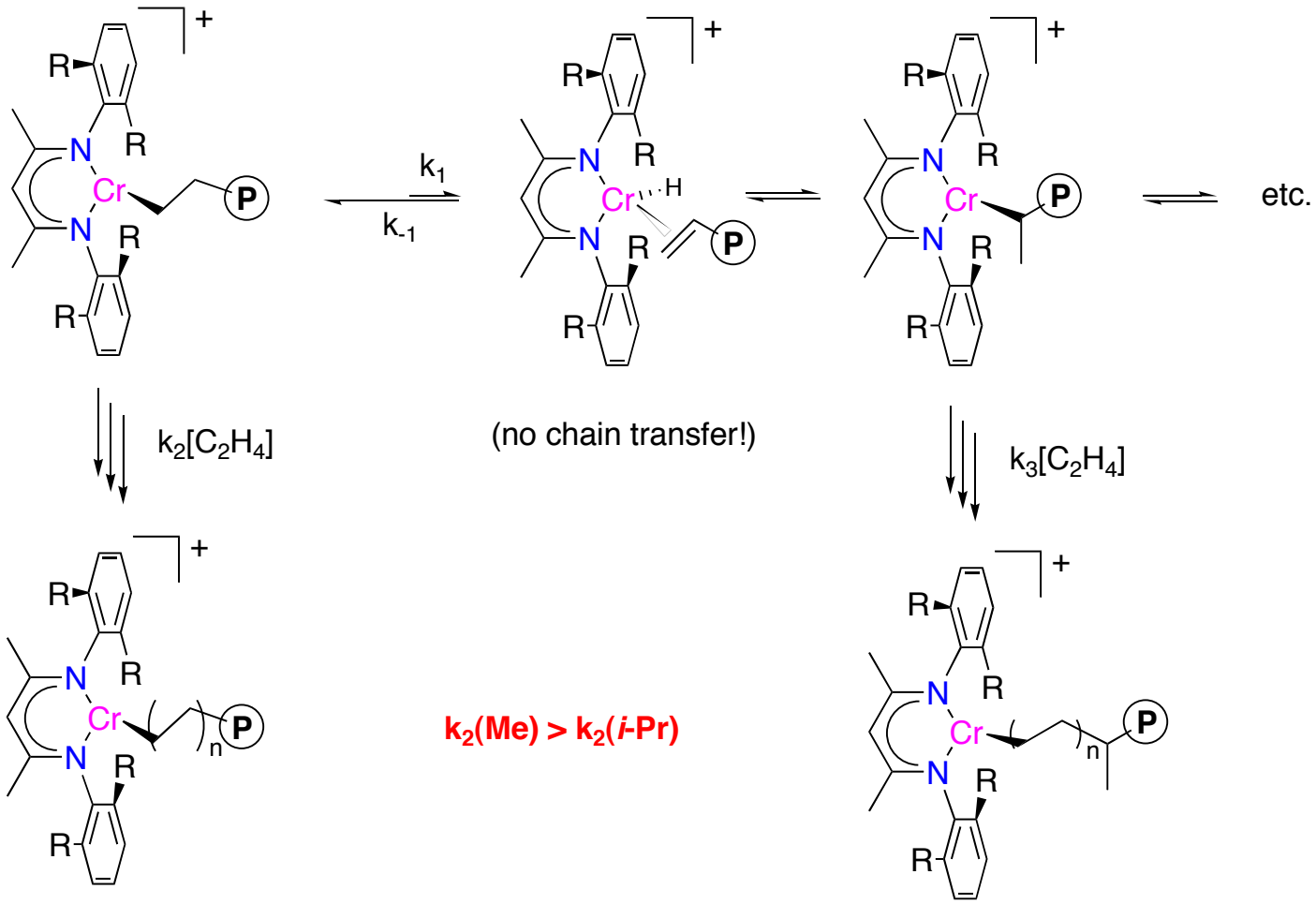

R = Me

R = *i*-Pr

P, T effect on chain walking - Me-branches counted by ^{13}C NMR

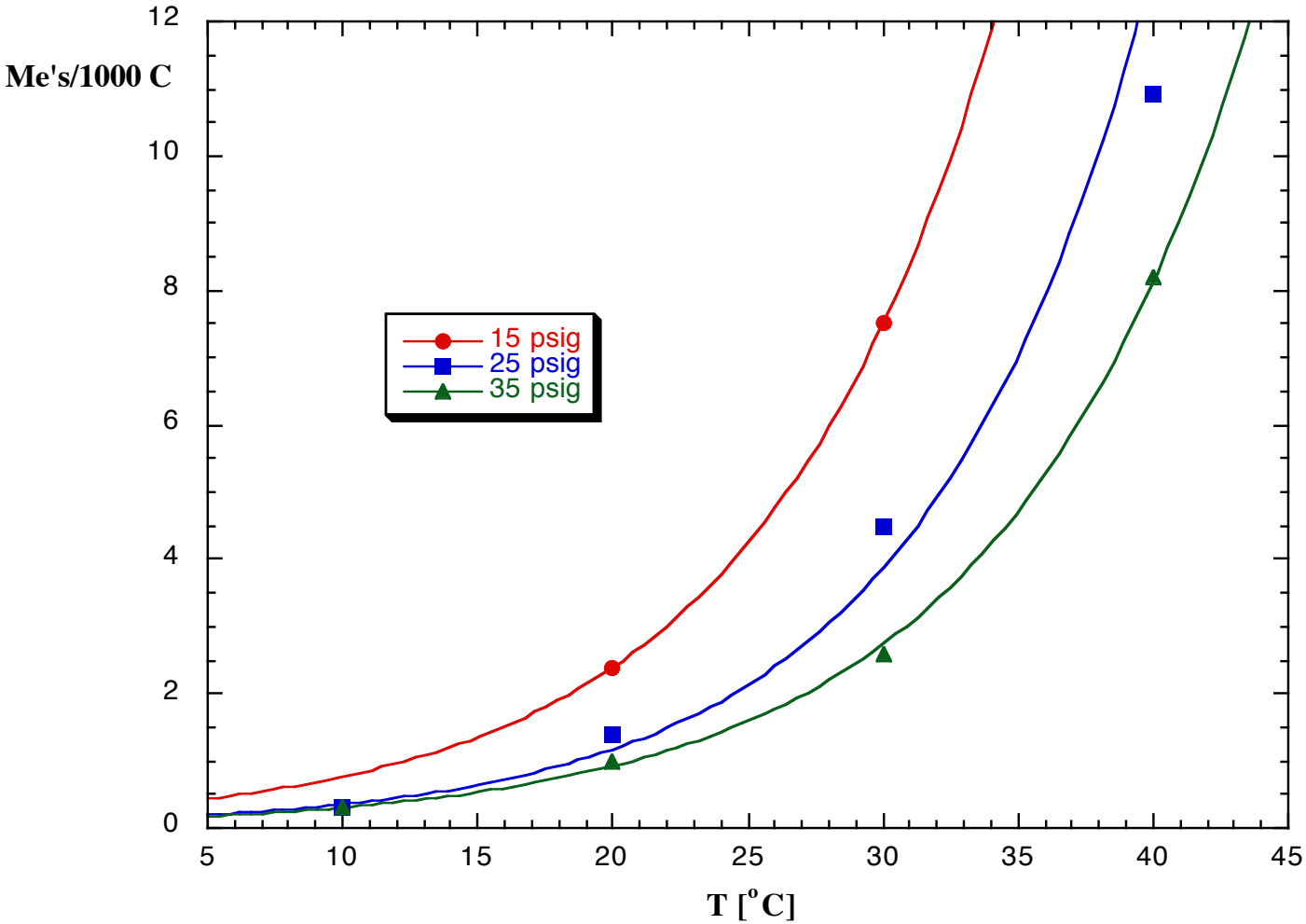

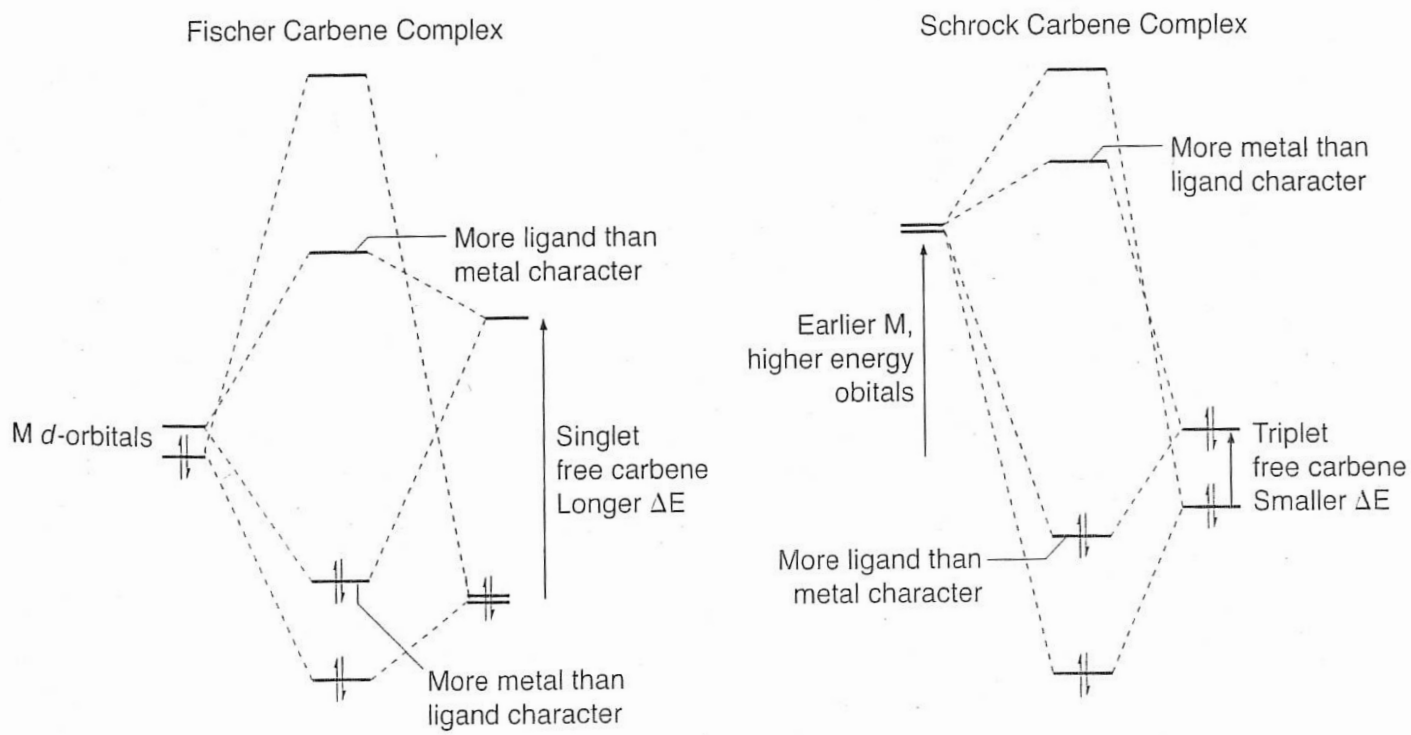

Figure 13.3. Molecular orbital diagram for Fischer and Scrock carbene complexes.

From J. Hartwig, *Organotransition Metal Chemistry*

Scheme 1

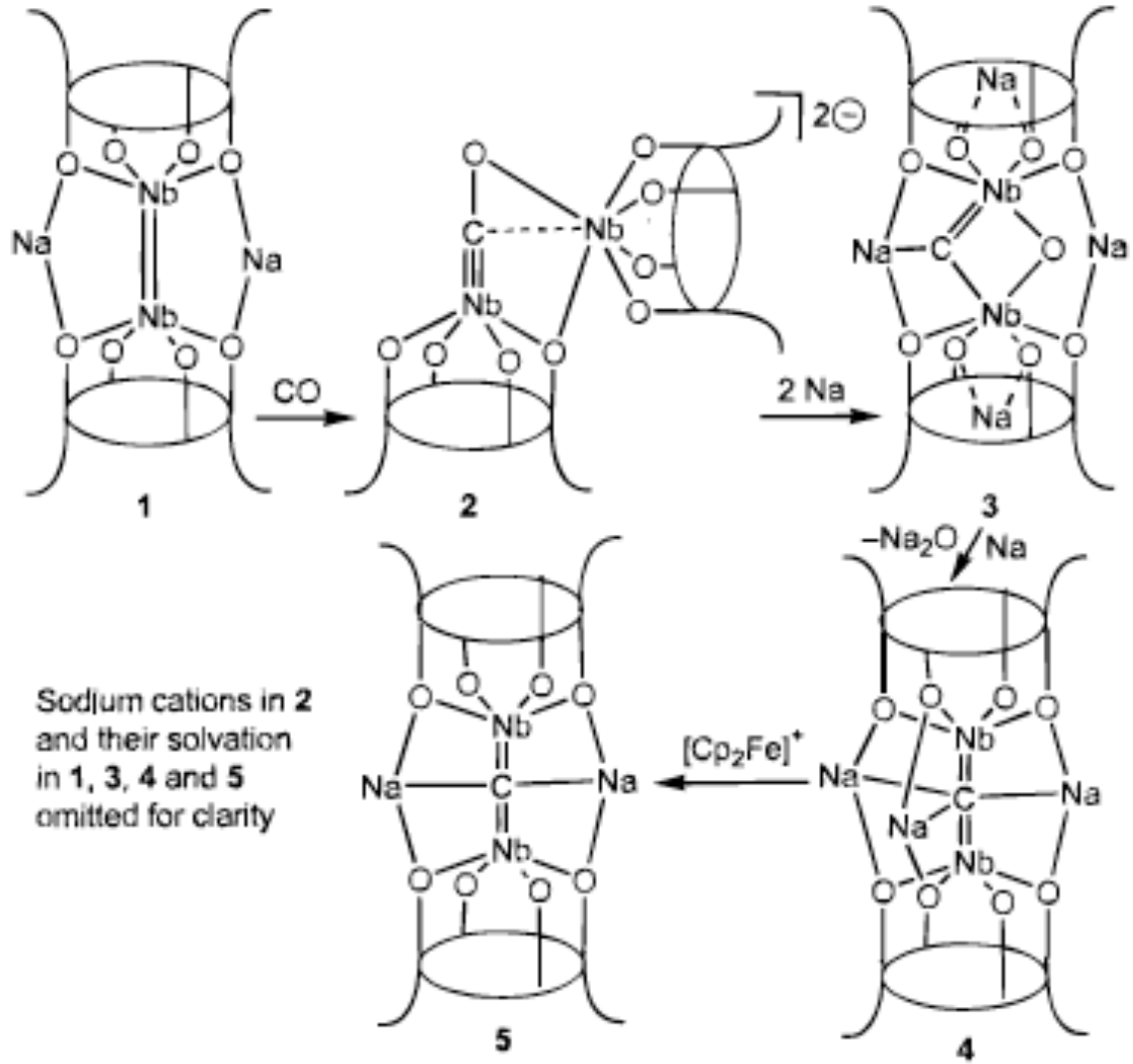

C. Floriani et al., *J. Am. Chem. Soc.* **2000**, *122*, 538

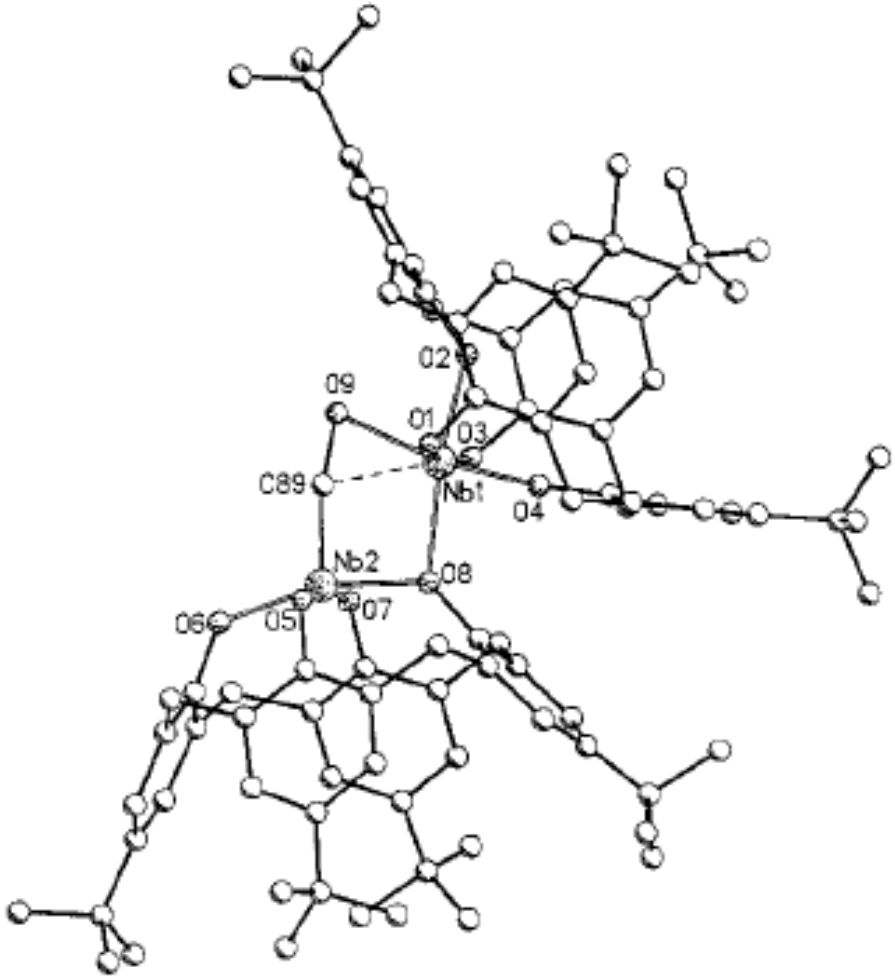

Figure 1. A plot showing one of the two dianionic dimers of compound **2**. Selected bond distances (Å) and angles (deg): Nb2−C89, 1.83(1); C89−O9, 1.32(1); Nb1−C89, 2.22(1); Nb1−O9, 2.154(7); Nb1···Nb2, 3.123(2); Nb2−C89−O9, 169(1).

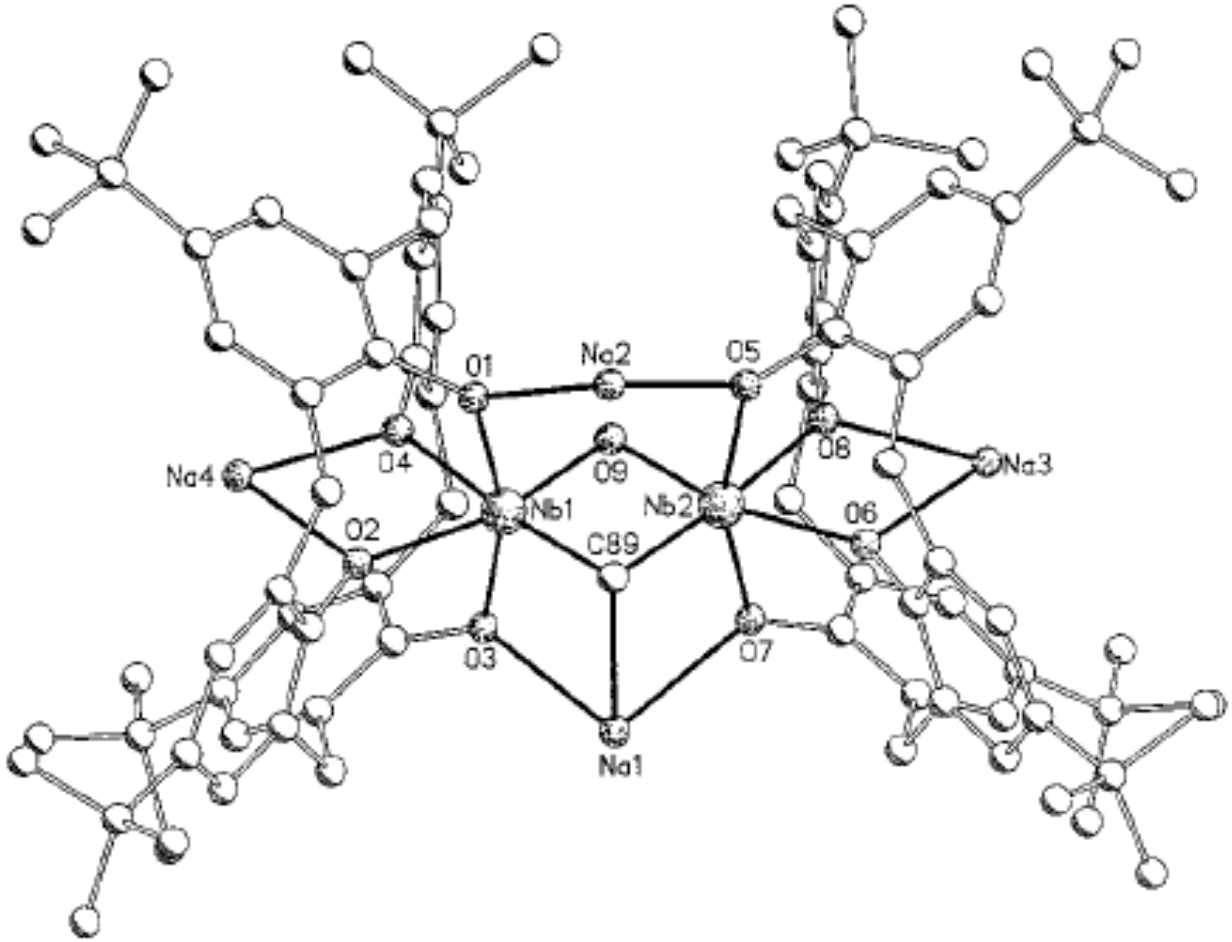

Figure 2. A view of compound **3** (solvent molecules omitted). Selected bond distances (Å) and angles (deg): Nb1−C89, 1.966(5); Nb2−C89, 1.968(5); Nb1−O9, 1.945(3); Nb2−O9, 1.939(3); C89···O9, 2.696(6); Nb1···Nb2, 2.8302(8); Na1−C89, 2.625(5); Nb1−C89−Nb2, 92.0(2).

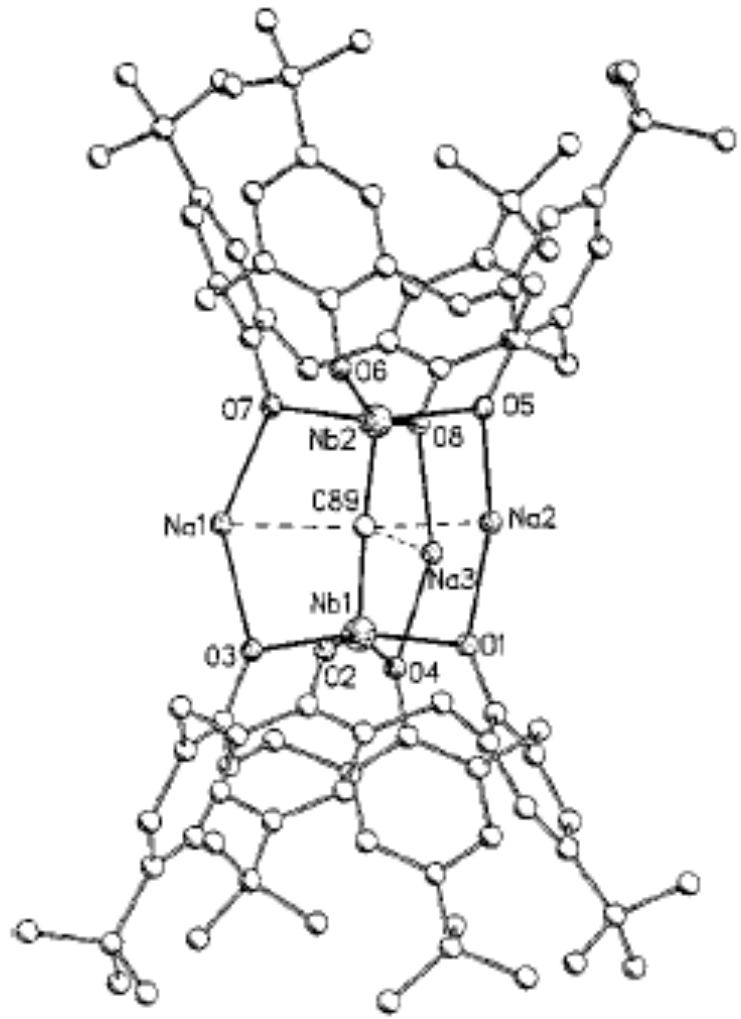

Figure 3. A view of compound **4** (solvent molecules omitted). Selected bond distances (Å) and angles (deg): Nb1−C89, 1.925(4); Nb2−C89, 1.919(3); Na1−C89, 2.698(4); Na2−C89, 2.745(4); Na3−C89, 2.876(4); Nb1−C89−Nb2, 173.9(2).

Halpern's study of hydrogenation catalysis w/ Wilkinson's catalyst

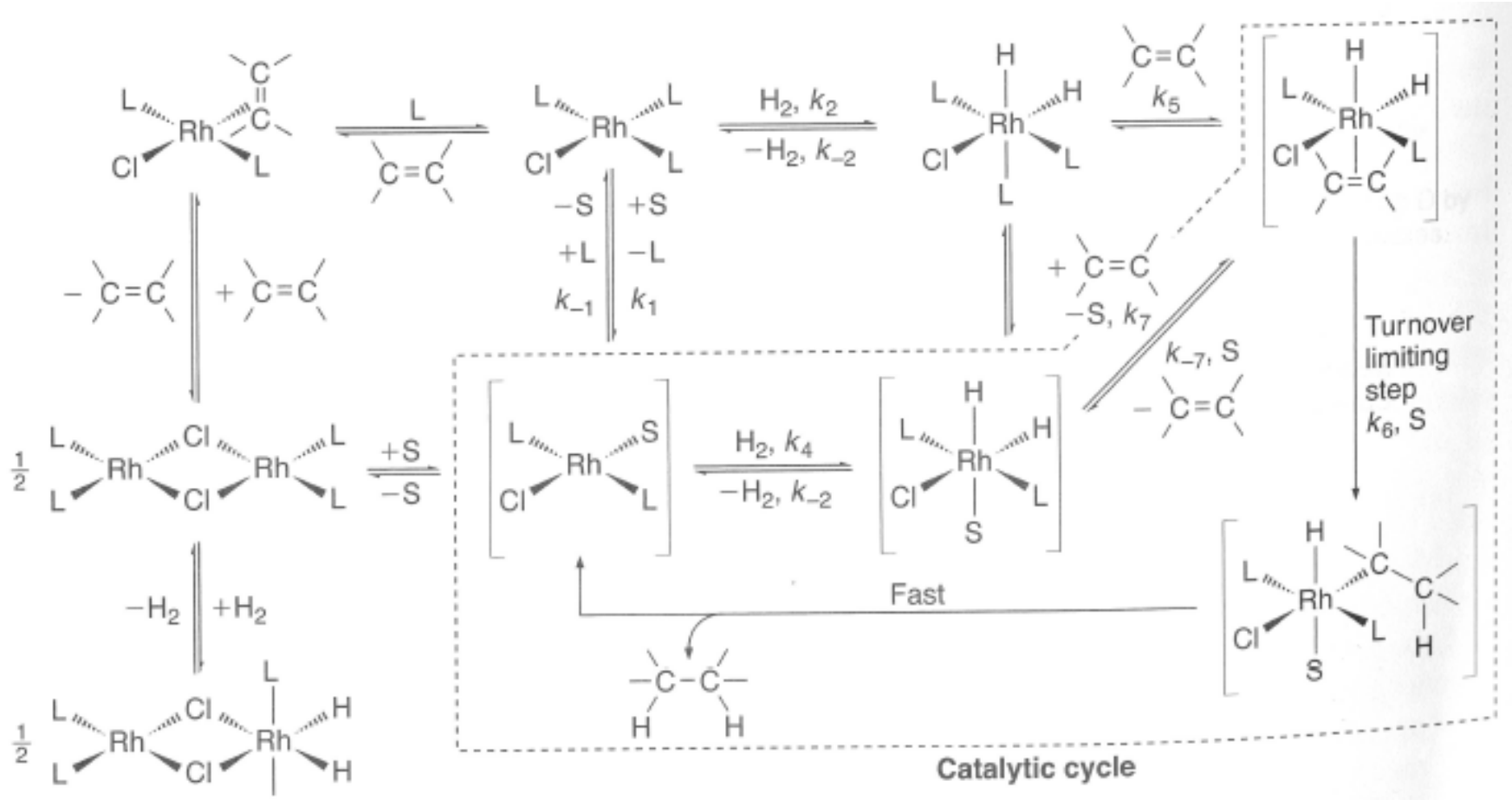

From John Hartwig, *Organotransition Metal Chemistry - ….*

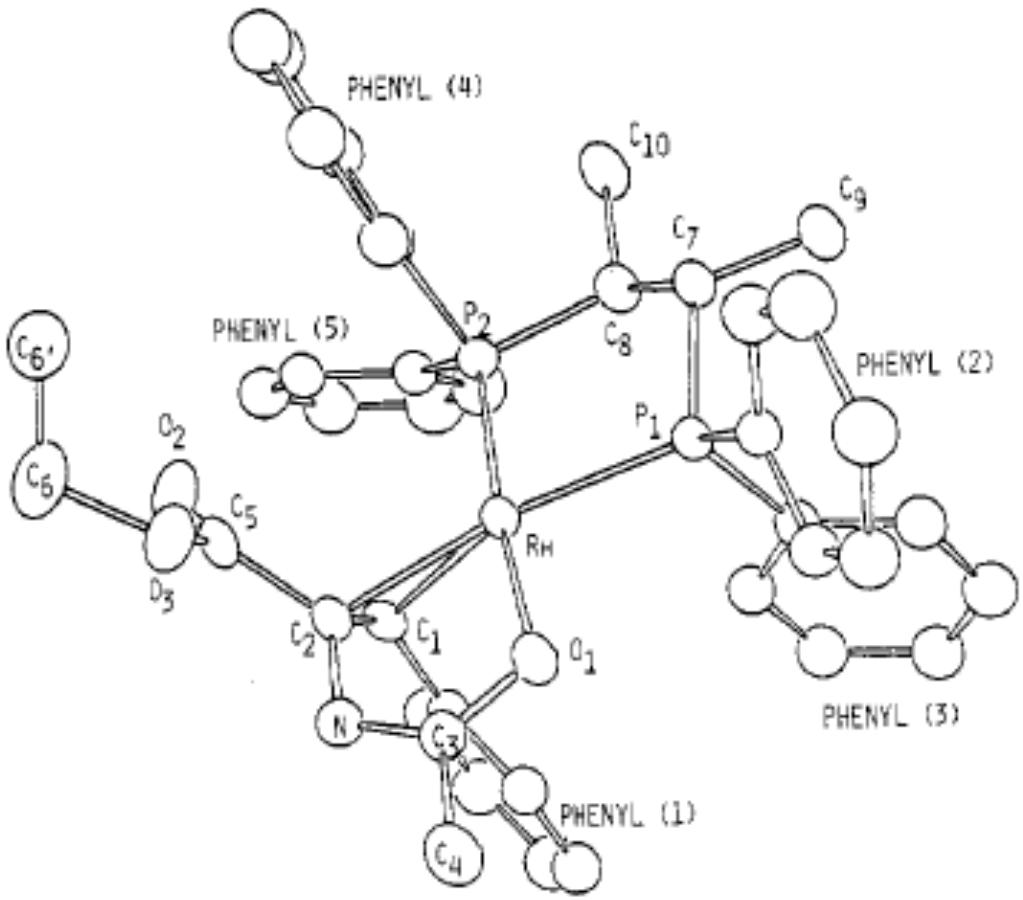

Figure 1. Structure of $[Rh(S,S\text{-chiraphos})(EAC)]^+$. Selected bond lengths (Å): $Rh-P_1$, 2.289 (2); $Rh-P_2$, 2.232 (2); $Rh-O_1$, 2.128 (5); $Rh-C_1$, 2.197 (8); $Rh-C_2$, 2.171 (8). Selected bond angles (deg): P_1-Rh-P_2, 83.1 (1); P_1-Rh-O_1, 89.8 (2); P_1-Rh-C_1, 147.3 (3); P_1-Rh-C_2, 167.9 (2); P_2-Rh-O_1, 168.2 (2); P_2-Rh-C_1, 93.1 (2); P_2-Rh-C_2, 109.0 (2); O_1-Rh-C_1, 98.0 (3); O_1-Rh-C_2, 78.0 (3); C_1-Rh-C_2, 36.9 (4).

Attempted synthesis of a 'base-free' cation .... almost!

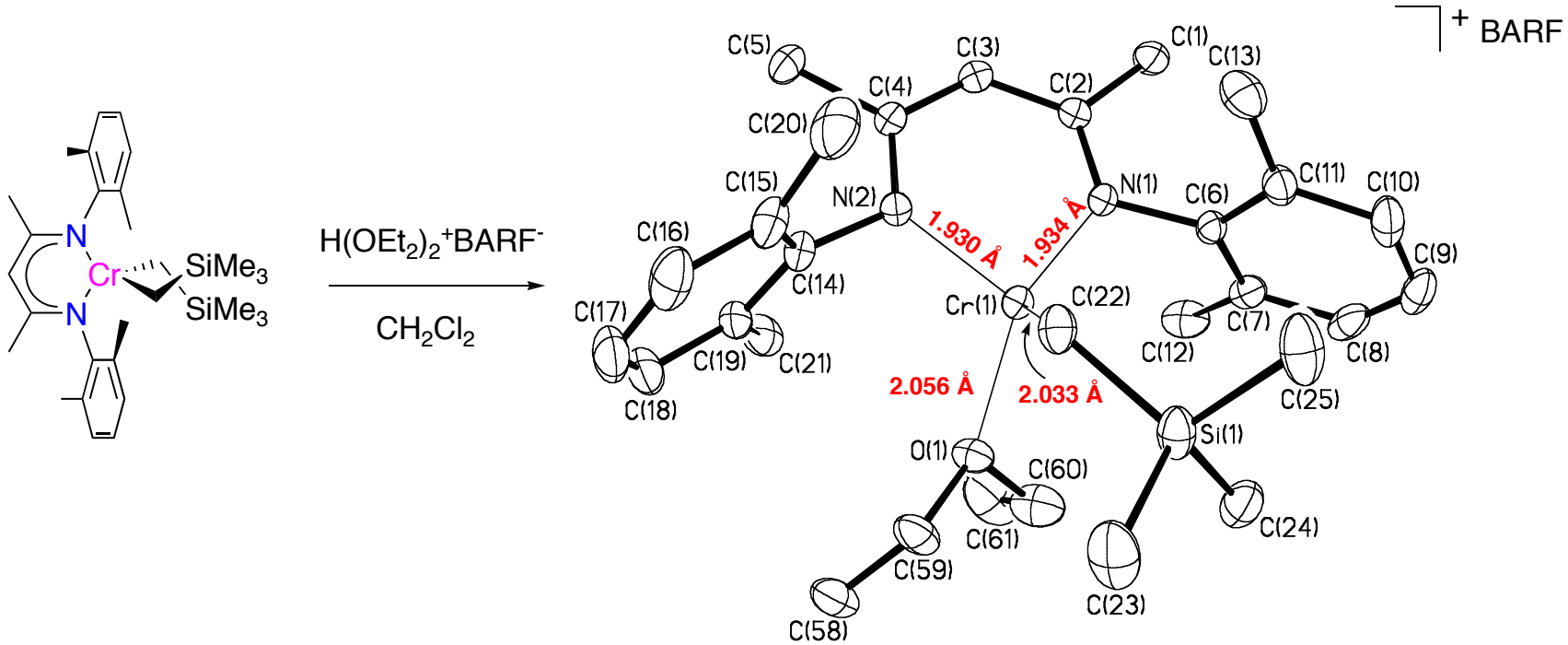

L. A. MacAdams et al, *J. Am. Chem. Soc*. **2005**, *127*,1082

Four-coordinate alkyl cation is active without a cocatalyst

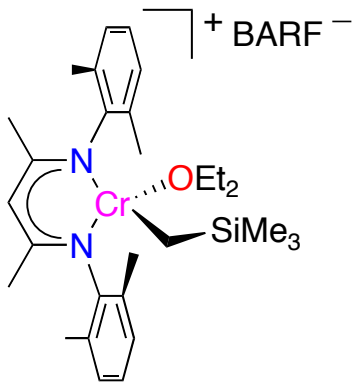

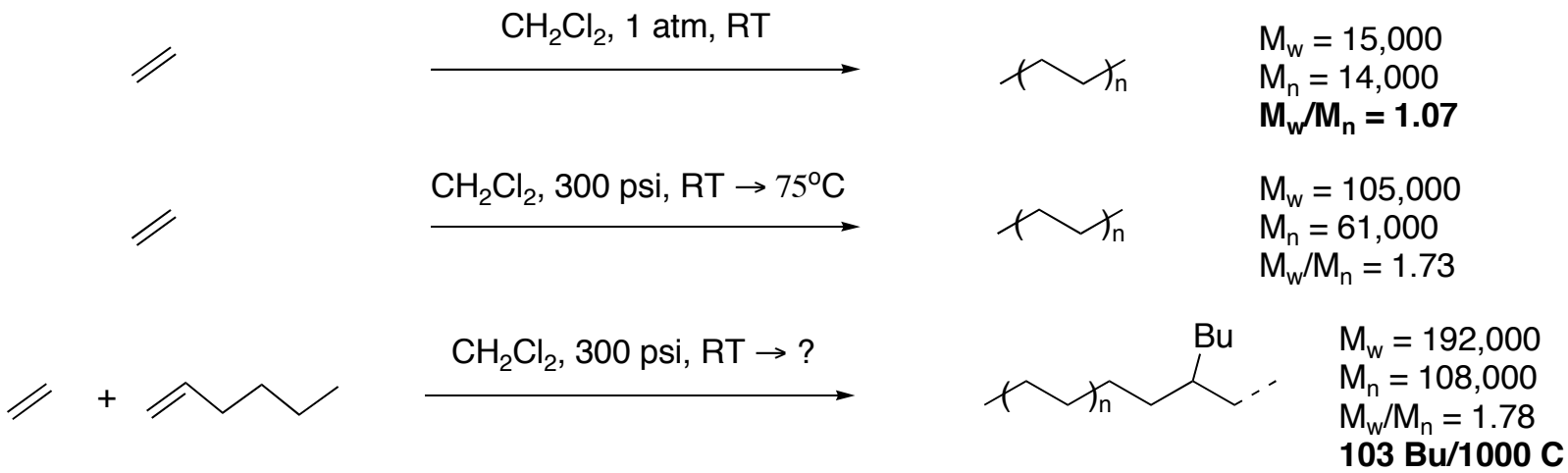

Isotopic Perturbation of Stereochemistry

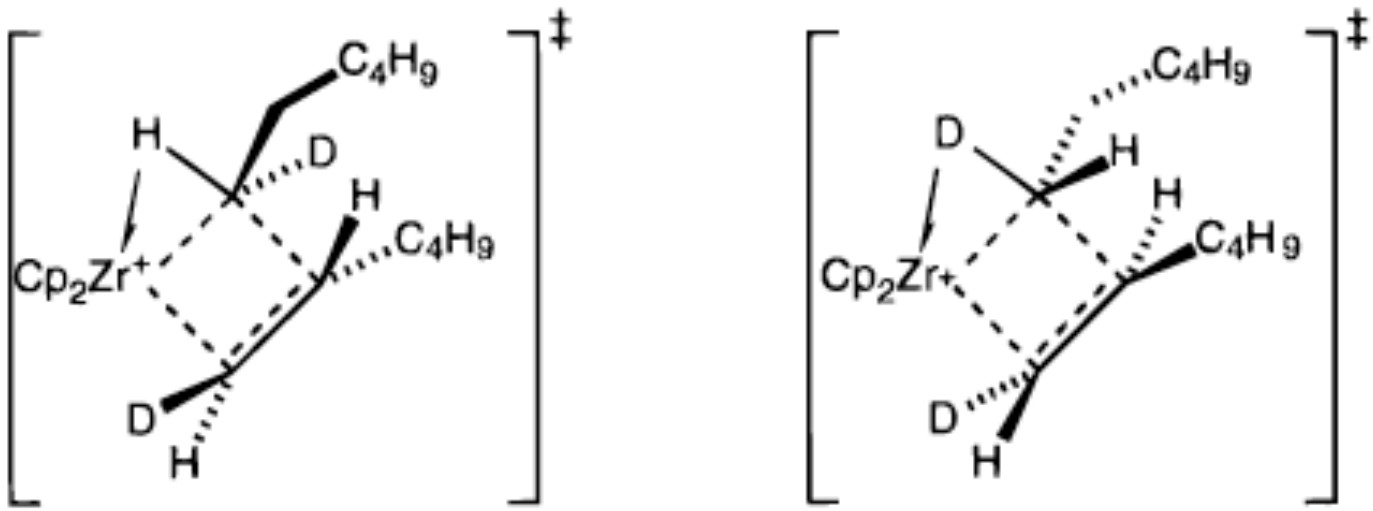

α-H Agostic, More Stable
⟶ *Erythro* Product

α-D Agostic, Less Stable
⟶ *Threo* Product

Figure 5. Stereochemistry of transition states involving α-H and α-D agostic interactions for the hydrodimerization of (*E*)-1-hexene-d_1 with MAO-activated Cp_2ZrCl_2.

R.H. Grubbs and G. W. Coates, *Acc. Chem. Res*. **1996**, *29*, 85

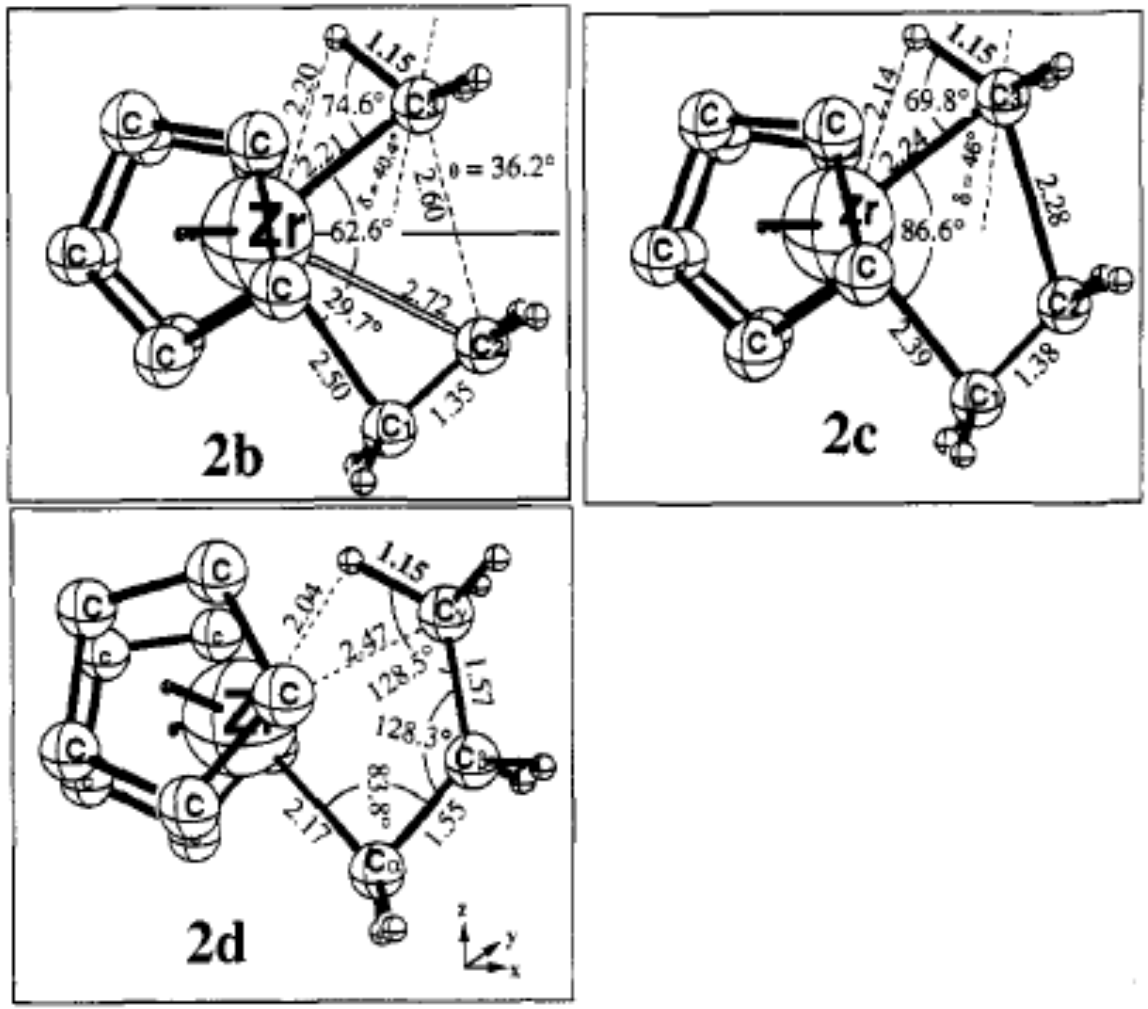

Figure 7. Optimized structures from the insertion of ethylene into zirconocene **2a**: (A) the π-complex, **2b**; (B) the transition state, **2c**; (C) the direct product, **2d**. The Cp ring hydrogens have been omitted for clarity.

T. Ziegler, *Organometallics*, **1994**, *13*, 2252

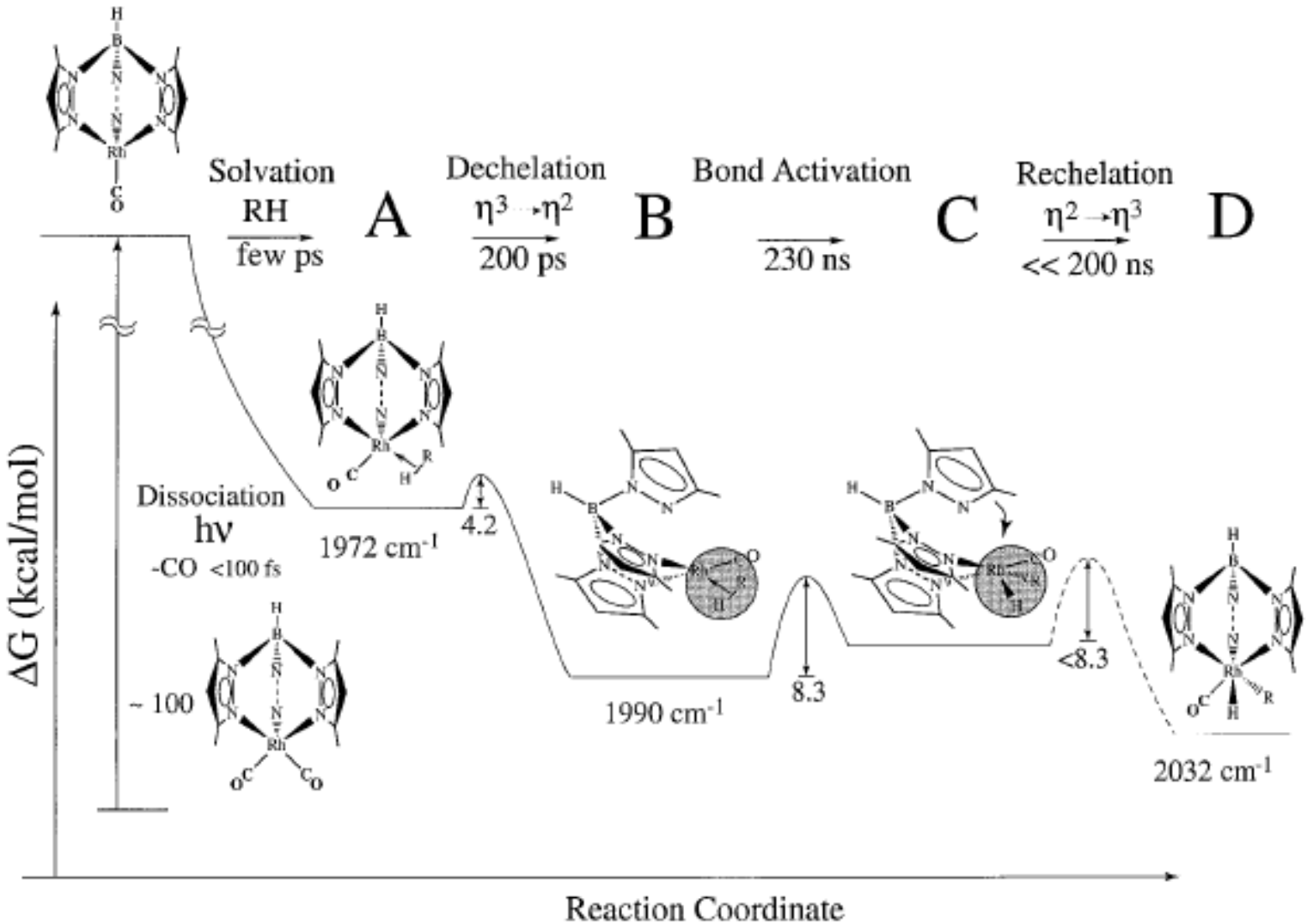

Fig. 6. Proposed mechanism and energy diagram for the C–H activation reaction of Tp*Rh(CO)$_2$ in alkane solution. These energy differences are estimates from separate ultrafast and nanosecond experiments. The stabilities of the intermediates are shown relative to each other and are not intended to be absolute.

S. E. Bromberg et al. *Science*, **1997**, *278*, 260

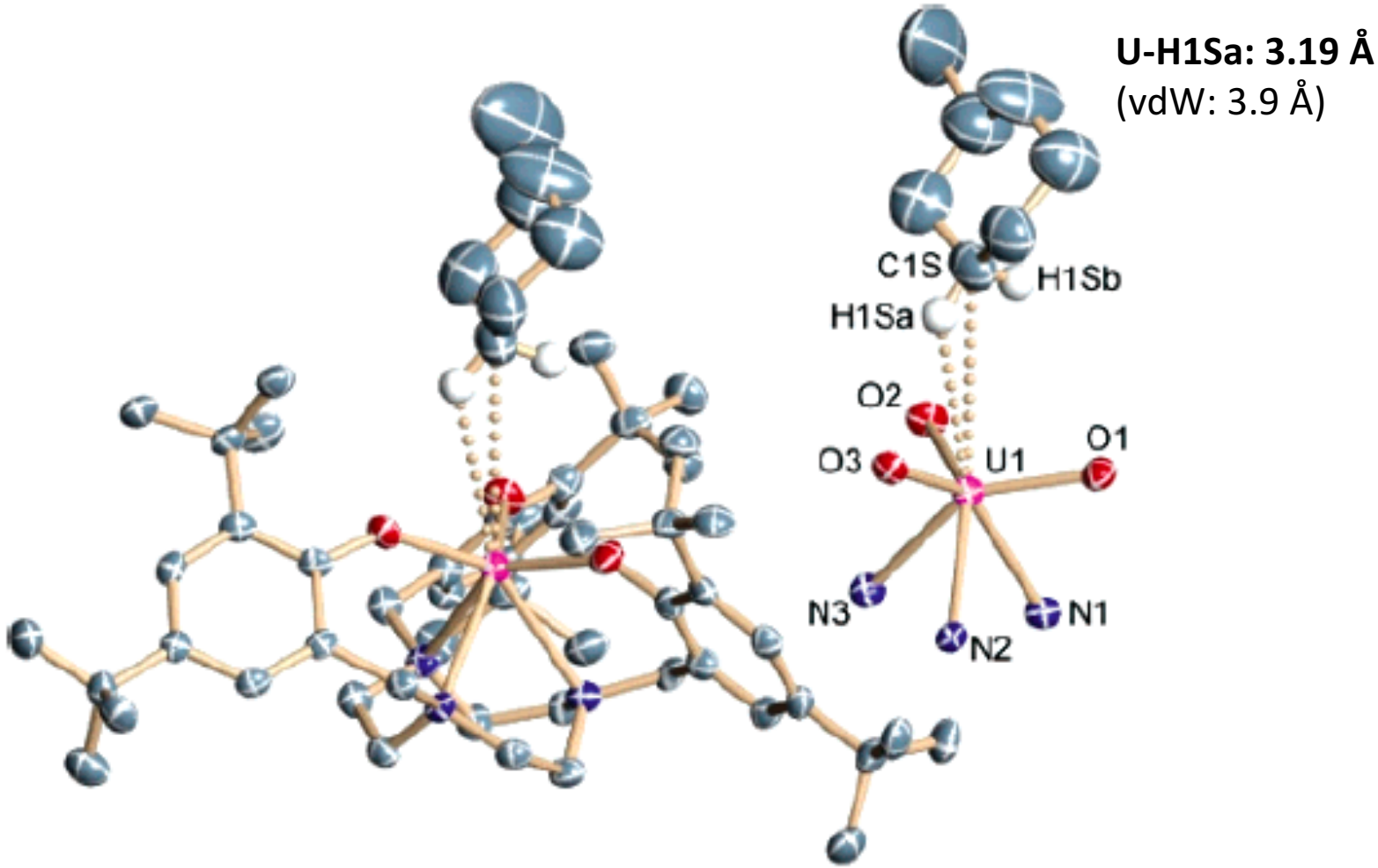

Figure 1. Solid-state molecular structure of $[((ArO)_3tacn)U(^{Me}cy\text{-}C6)]\cdot(^{Me}cy\text{-}C6)$ (**1c**), with dotted lines emphasizing the η^2-H,C mode. Hydrogen atoms and cocrystallized solvent molecule are omitted for clarity; thermal ellipsoids at 50% probability.

I. Castro-Rodriguez et al, *J. Am. Chem. Soc.* **2003**, *125*, 15734

Fig. 3 (A) Displacement ellipsoid plots (30% probability) for the cationic components of complexes 1, 2, and 3 in the solid state.

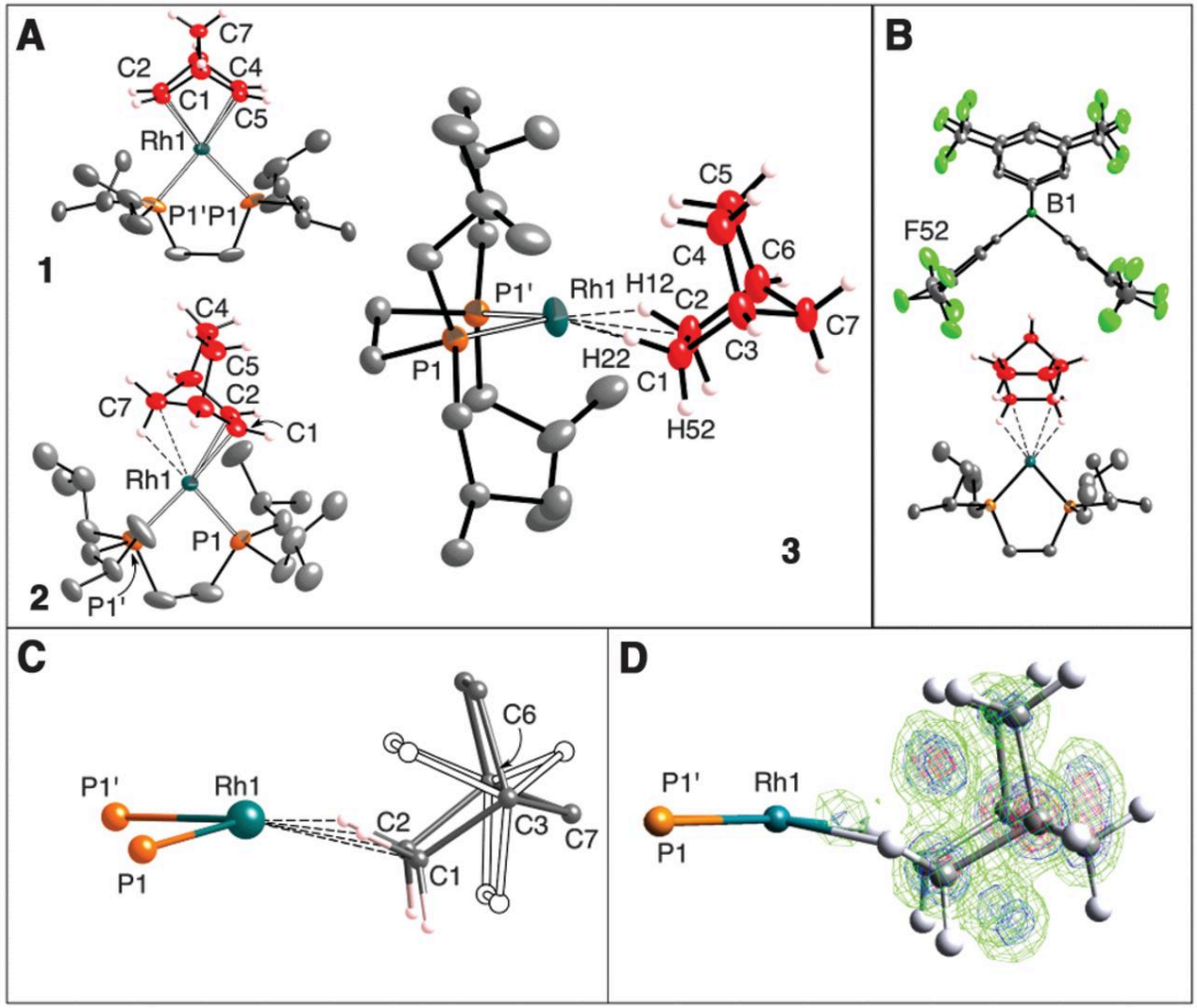

Sebastian D. Pike et al. Science 2012;337:1648-1651

Published by AAAS

Mechanism of an intramolecular O_2-insertion

*(*see *Angew. Chem. Int. Ed.* **1999***, 38,* 166*)*

IR (toluene, - 50°C):
$\nu_{O\text{-}O}$: 1027 cm^{-1} ($^{16}O_2$)
$\nu_{O\text{-}O}$: 969 cm^{-1} ($^{18}O_2$)

$\nu_{Cr=O}$: 922 cm^{-1}
μ_{eff} = 2.6(1) μ_B
Cr=O: 1.576(3) Å
Cr-O: 1.844(3) Å

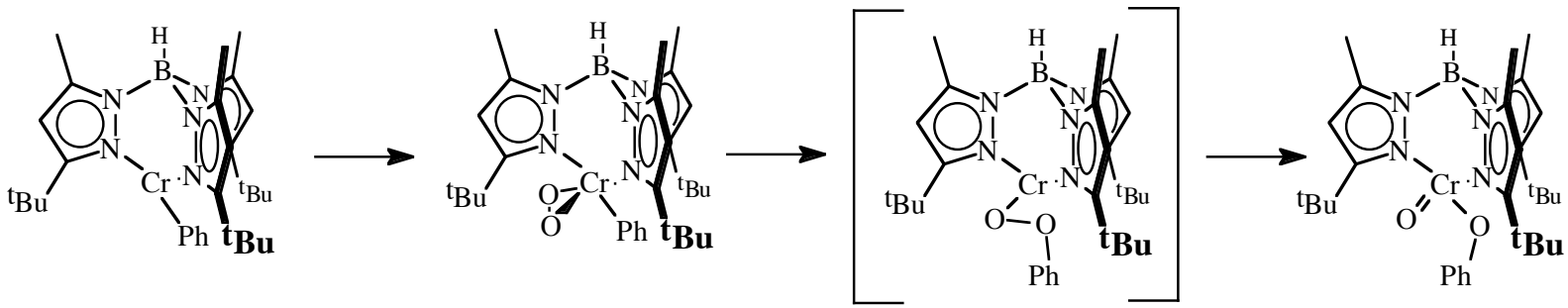

Spectroscopically observable superoxo intermediate.
<u>Proposed</u> to exhibit η^2-coordination (side-on bonding), based on the preference of Cr(III) for octahedral coordination

A <u>stable</u> Cr(IV) oxo complex

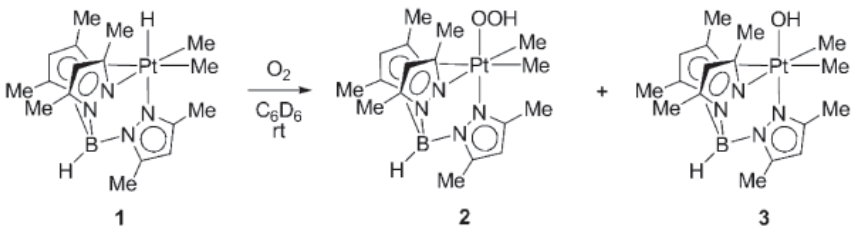

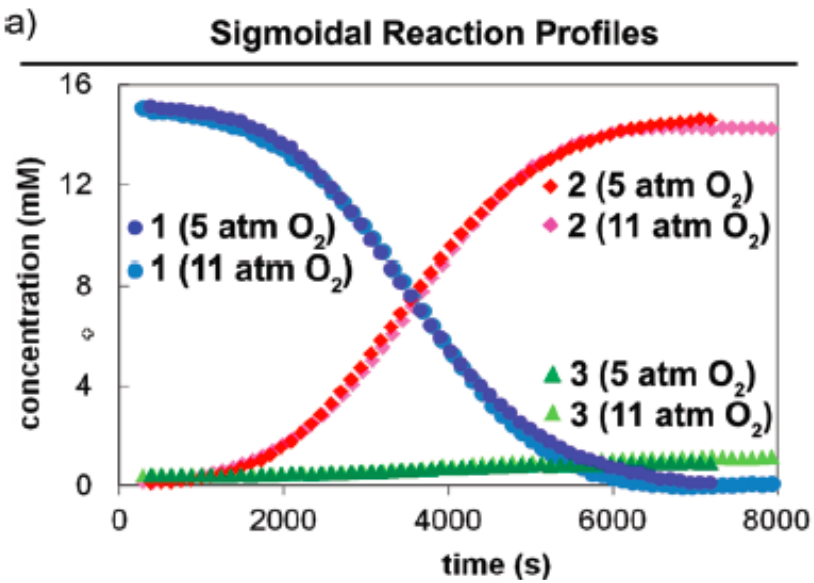

initiation

(1) AIBN → 2 In•

(2) In• + O_2 → InOO•

(3) InOO• + Pt-H → InOOH + Pt•

R_i

propagation

(4) Pt• + O_2 → PtOO•

(5) PtOO• + Pt-H $\xrightarrow{k_p}$ PtOOH + Pt•

autocatalysis

(6) PtOOH + In• → PtOO• + In-H

termination

(7) PtOO• + (Pt / PtOH / PtOOH) $\xrightarrow{k_t}$ non-propagating products

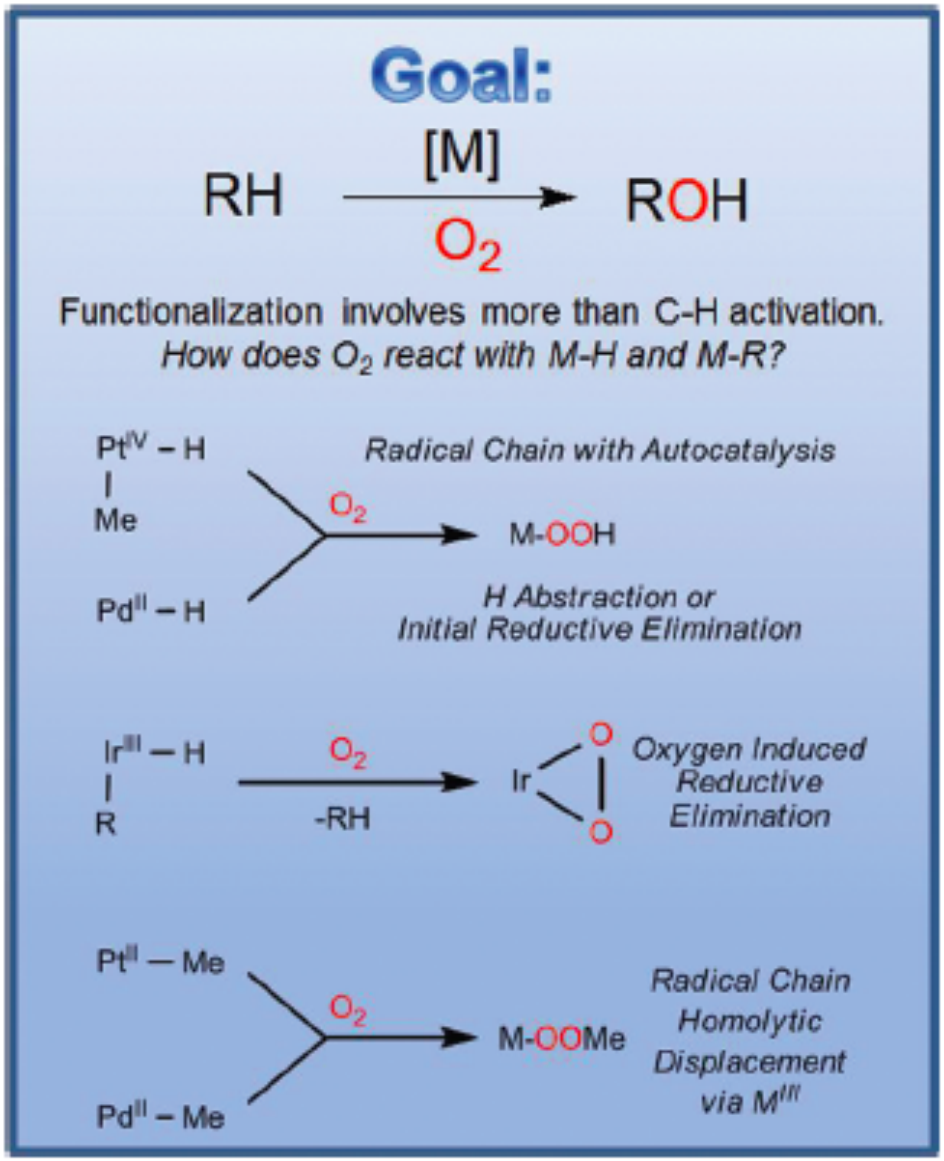

K. I. Goldberg, *Acc. Chem. Res*. **2012**, *45*, 899

(*a*) *Unit cell of* $(LiCH_3)_4(s)$

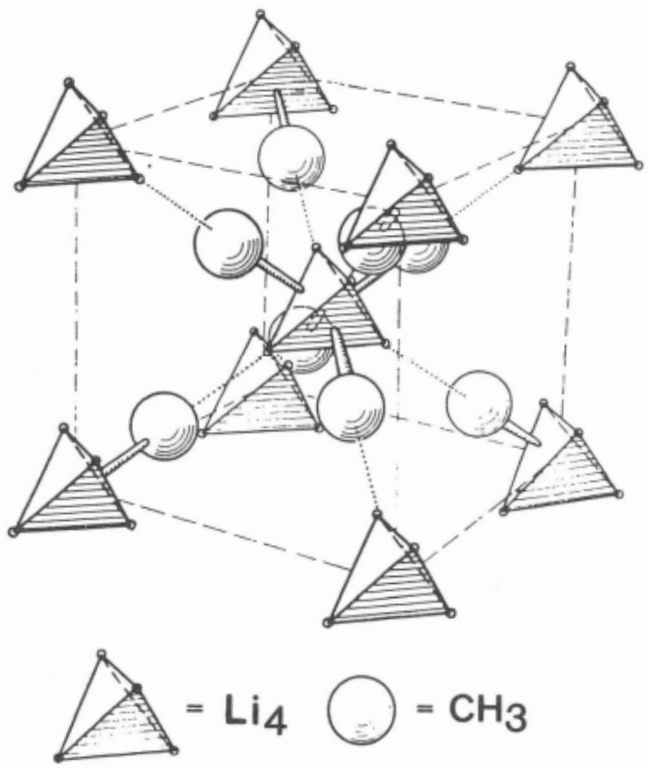

(*b*) *Schematic drawing of the unit* $(LiCH_3)_4$

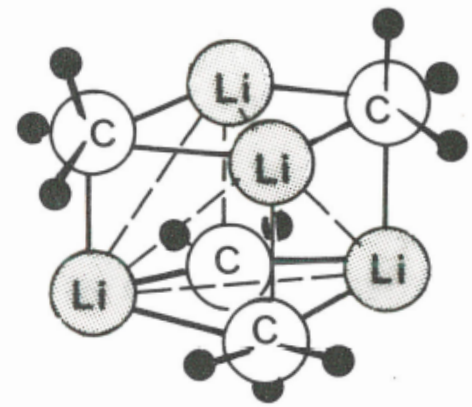

	$d(Li-C) = 231$ pm	$(LiCH_3)_4$
	$d(Li \cdot\cdot C) = 236$ pm	$(LiCH_3)_4$
	$d(Li-Li) = 268$ pm	$(LiCH_3)_4$
compare:	$d(Li-Li) = 267$ pm	$Li_2(g)$
	$d(Li-Li) = 304$ pm	$Li(m)$